Quantum dot optofluidic lasers and their prospects for biochemical sensing *and some gas sensing results*

Alper Kiraz

Department of Physics, Koç University

Fan Lab @ Michigan

Prof. Alexandr Jonas, İTÜ

Mehdi Aas
Recent PhD Alumni

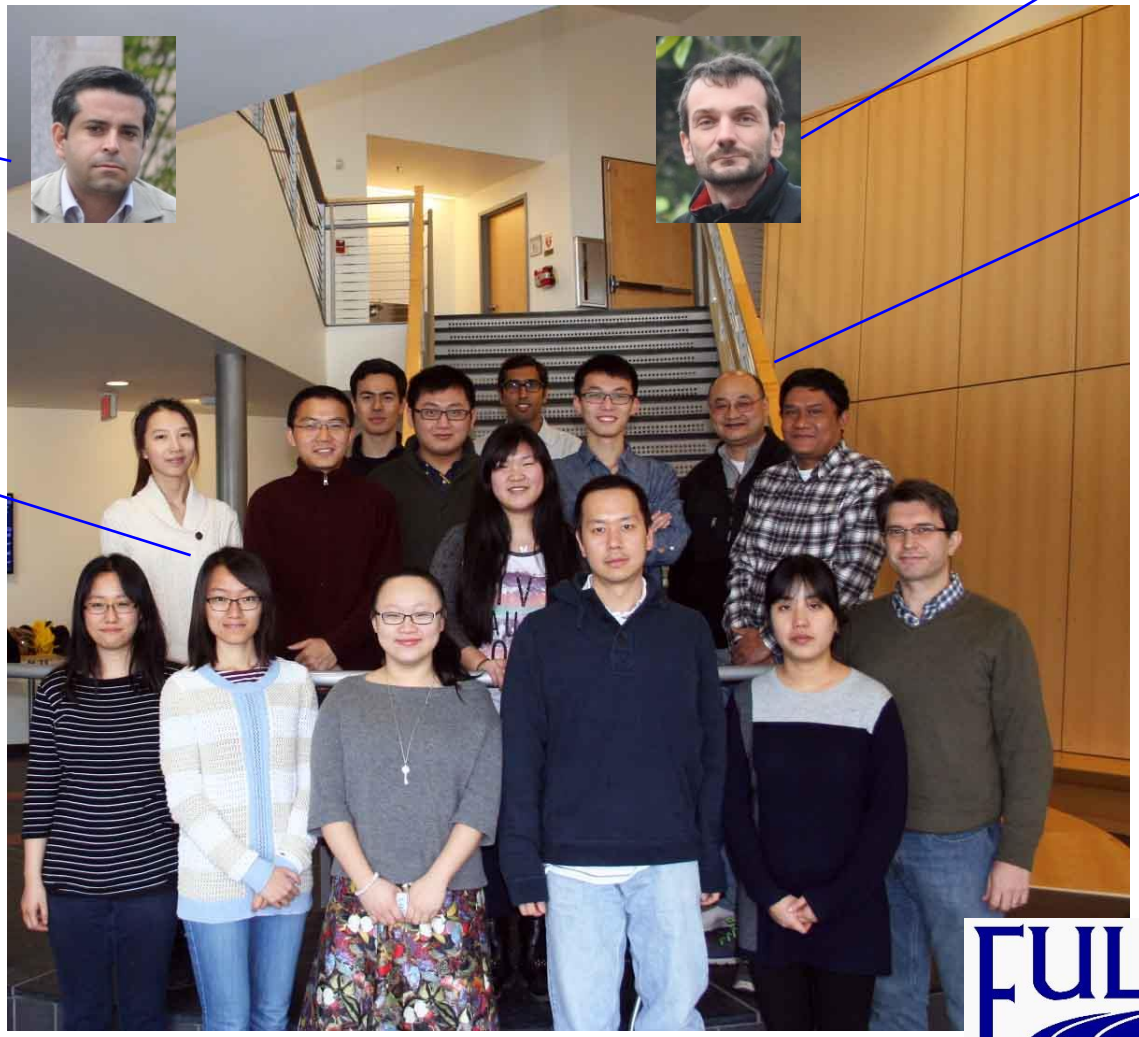

Prof. Sherman Fan

Qiushu Chen
PhD Student

FULBRIGHT

Our Lab @ Koç

Prof. Necmettin Kılınç,
Niğde U.

Assoc. Prof. Nevin Taşaltın,
TÜBİTAK MAM Materials Ins.

Prof. Yasin Karadağ,
Marmara U.

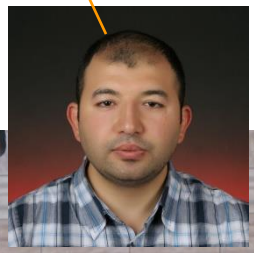

Mustafa Eryürek
PhD Student

Dr. Suman Anand
Post-Doctoral Researcher

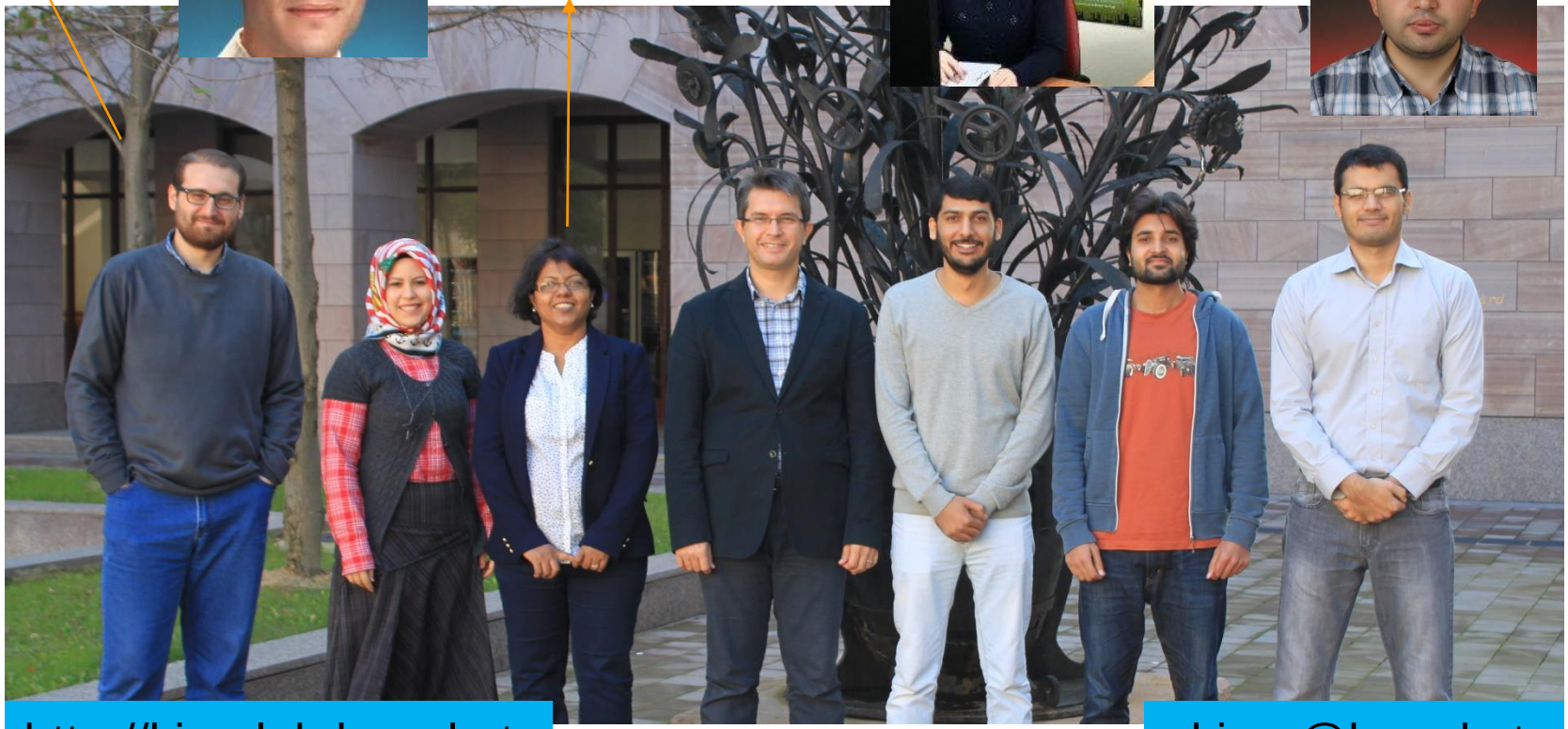

http://kirazlab.ku.edu.tr

akiraz@ku.edu.tr

Acknowledgements

TÜBİTAK

110T803,114F253,115S120,
115F446

Q.C. and X.F. acknowledge the support from the National Institutes of Health (1R21EB016783).

Outline

Optofluidic Lasers

- Potential of optofluidic lasers for biosensing
- Optofluidic lasing with aqueous quantum dots
- Optofluidic FRET lasing with aqueous quantum dots as donors

Gas Sensing With Elastic Microresonators

- Humidity sensinf with polymer microdisk microresonators
- Hydrogen sensing with polymer microdisk microresonators

POTENTIAL OF OPTOFLUIDIC LASERS FOR BIOSENSING

Microplate Reader

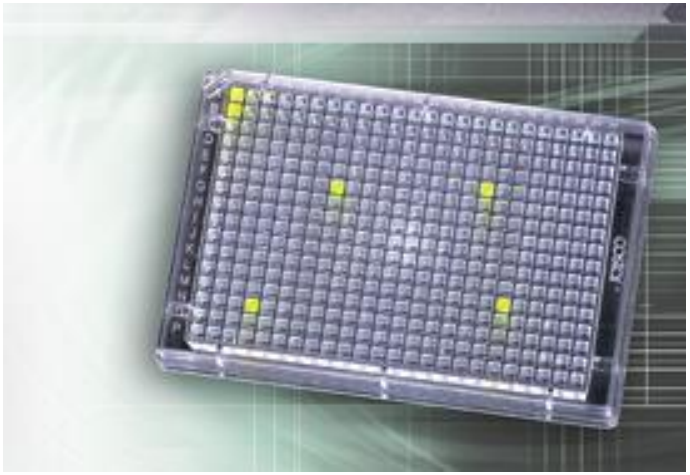

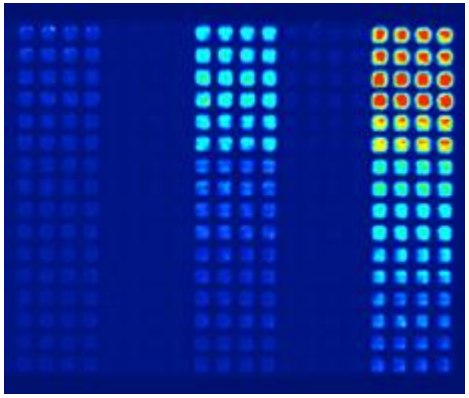

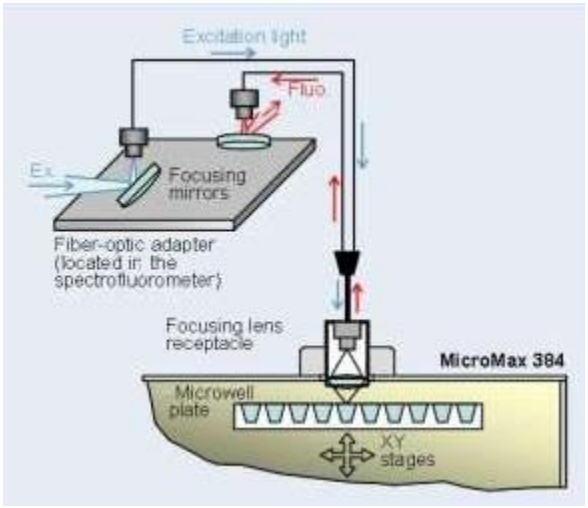

Fluorescence Assay

Fluorescence microplate applications

Caspase Assays

- Live-cell assays
- Caspase-3/7 assays
- Other caspase substrates

Cell Proliferation

- DNA content
- DNA synthesis

Cell Signaling and Lipids

- Cholesterol
- Phosphate and pyrophosphatase
- Phosphatase
- Phospholipase

Cell Viability

- Mammalian cell assays (measuring reduction potential and membrane integrity)
- Bacteria and yeast assays

Enzyme Activity

- Phosphatases
- Phospholipases
- Proteases
- Other enzymes

β-Galactosidase Assays

- Assay kits
- β-gal substrates
- Glucosidase substrates

Ion Indicators

- Intracellular calcium
- Intracellular magnesium
- pH indicators

Metabolites and Analytes

- Metabolic assays
- Neurobiology assays
- Inflammation assays

Nucleic Acids

- dsDNA assays
- ssDNA assays
- RNA assays

Protein Quantitation

- CBQCA

Reactive Oxygen Species

- Oxidative stress

Viability Confirmation

- Multiplexed viability/cytotoxicity

https://www.thermofisher.com

FRET-Based Fluorescence Assay for ssDNA Detection

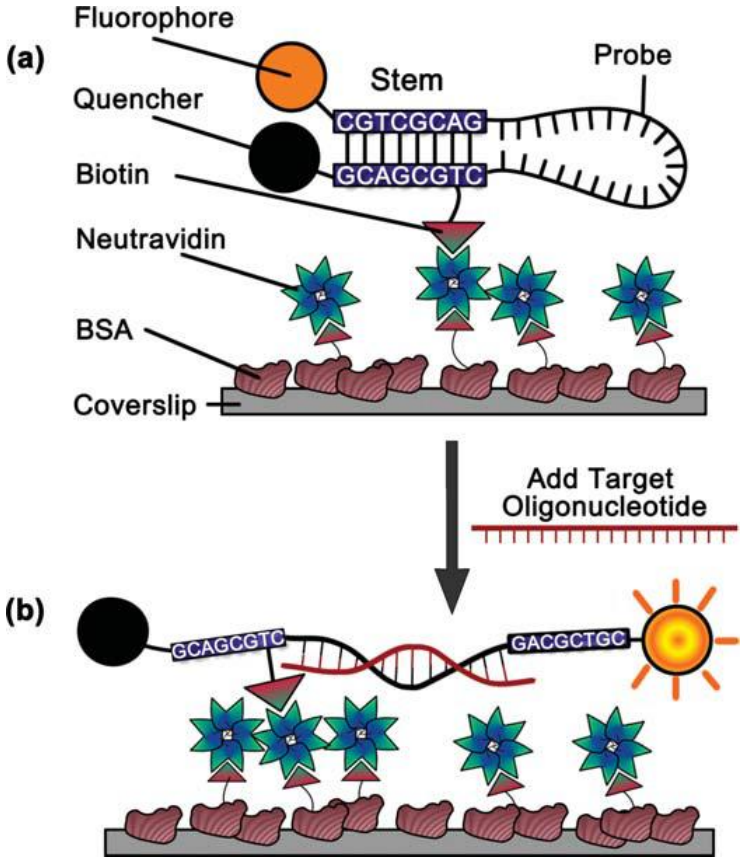

B. R. Schudel *et al*., Lab Chip 11, 1916 (2011)

Fluorescence Resonance Energy Transfer (FRET)

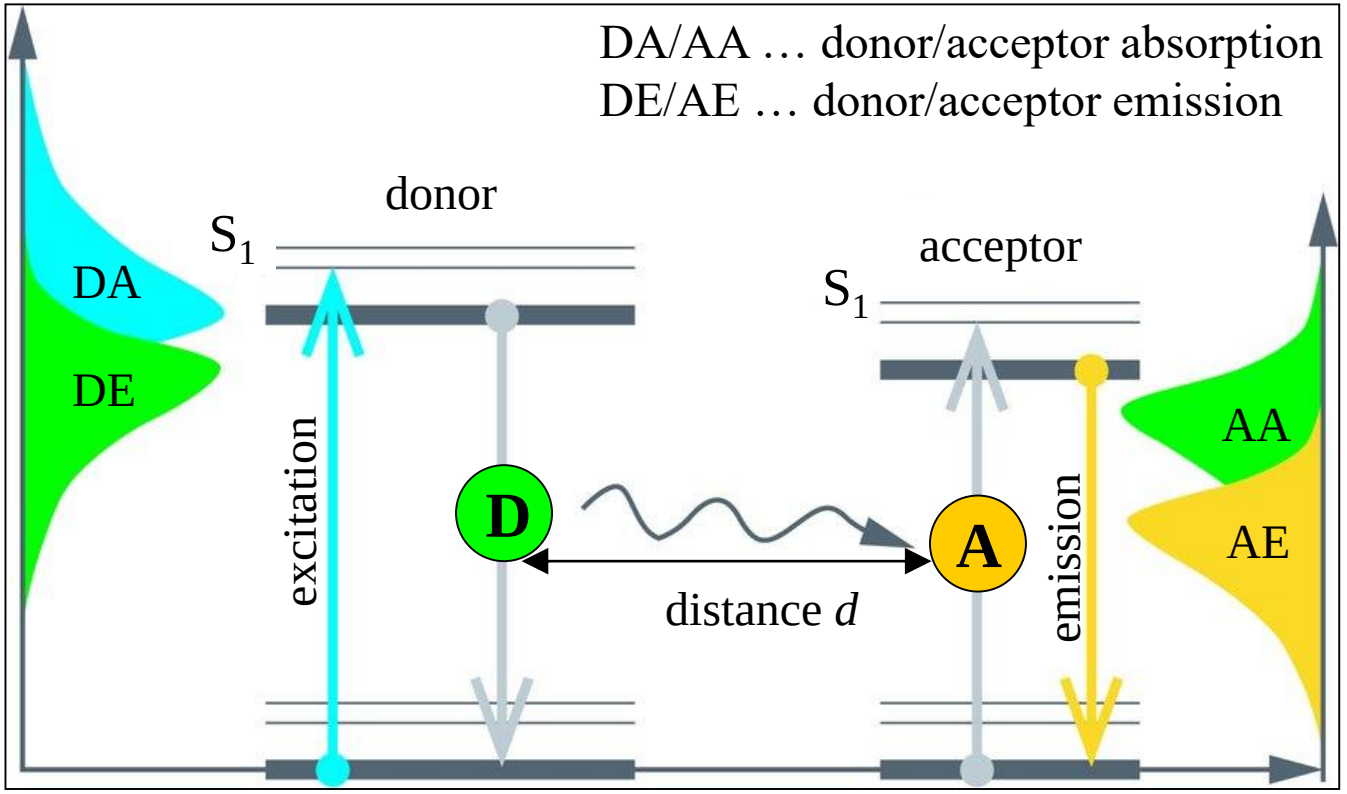

Non-radiative energy transfer between donor and acceptor due to spectral overlap DE/AA

Strongly distance-dependent → FRET efficiency

Typical Förster distance R_0: 2 – 10 nm

$$E_{FRET} = \frac{R_0^6}{R_0^6 + d^6}$$

Biosensing with Optofluidic Microlasers

Benefit from the high sensitivity of stimulated emission to perturbations in the gain medium and laser cavity

High signal to noise ratio in biological and chemical analysis

⇨ Biological sensing using FRET mechanism

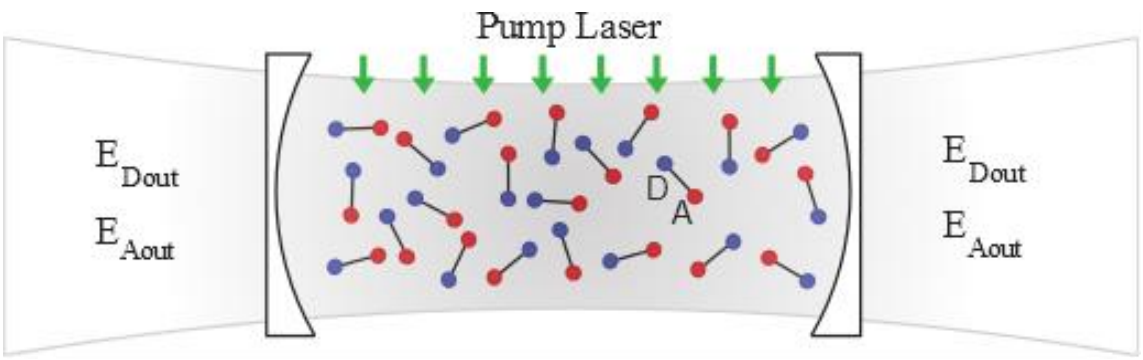

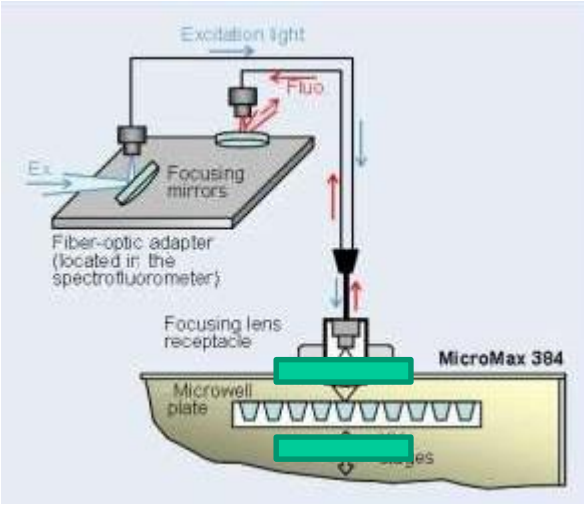

Biosensing with Optofluidic Microlasers

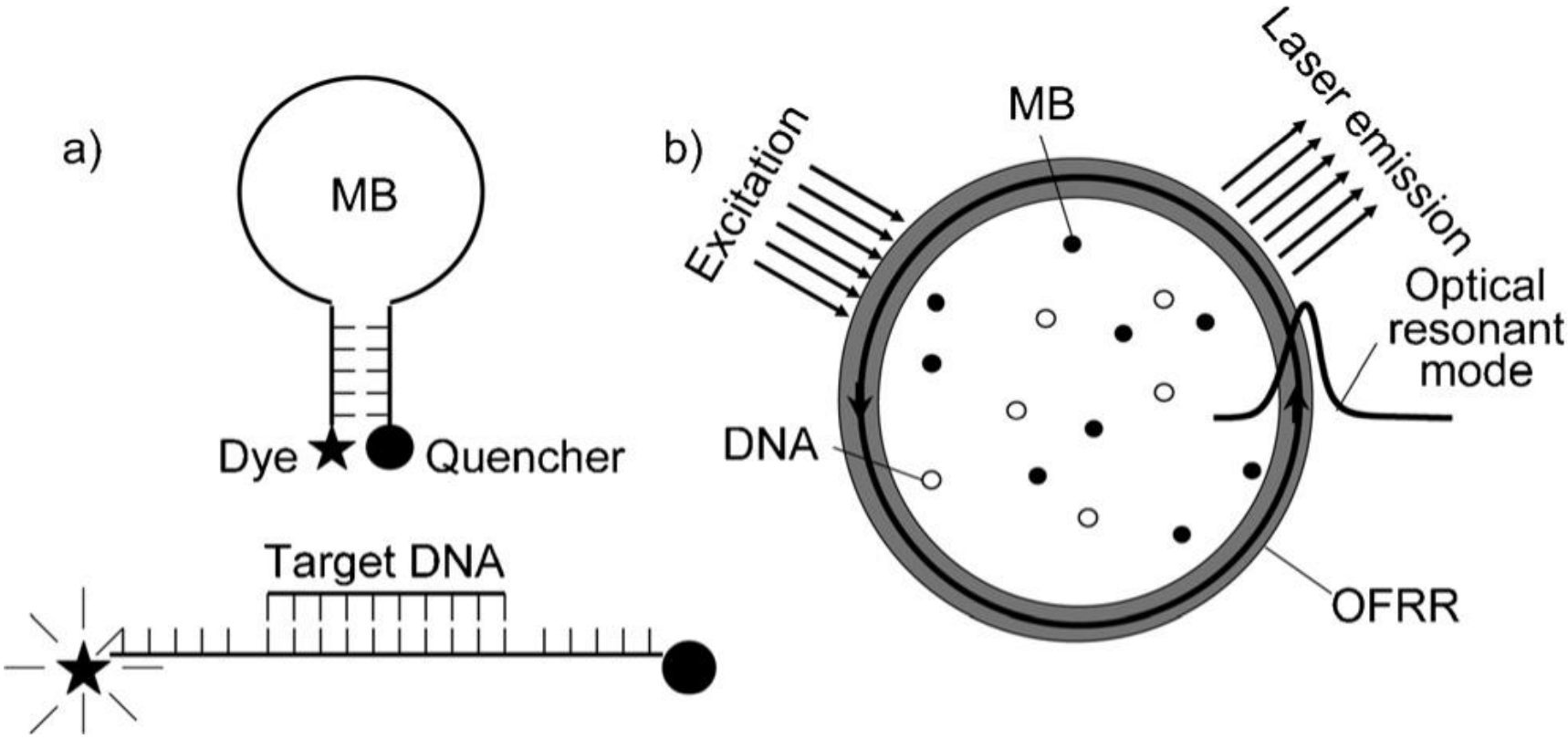

Y. Sun and X. Fan, Angew. Chem. Int. Ed. 51 (2012), 1236 - 1239

Ion-dependent Folding of the DNA Holliday Junction

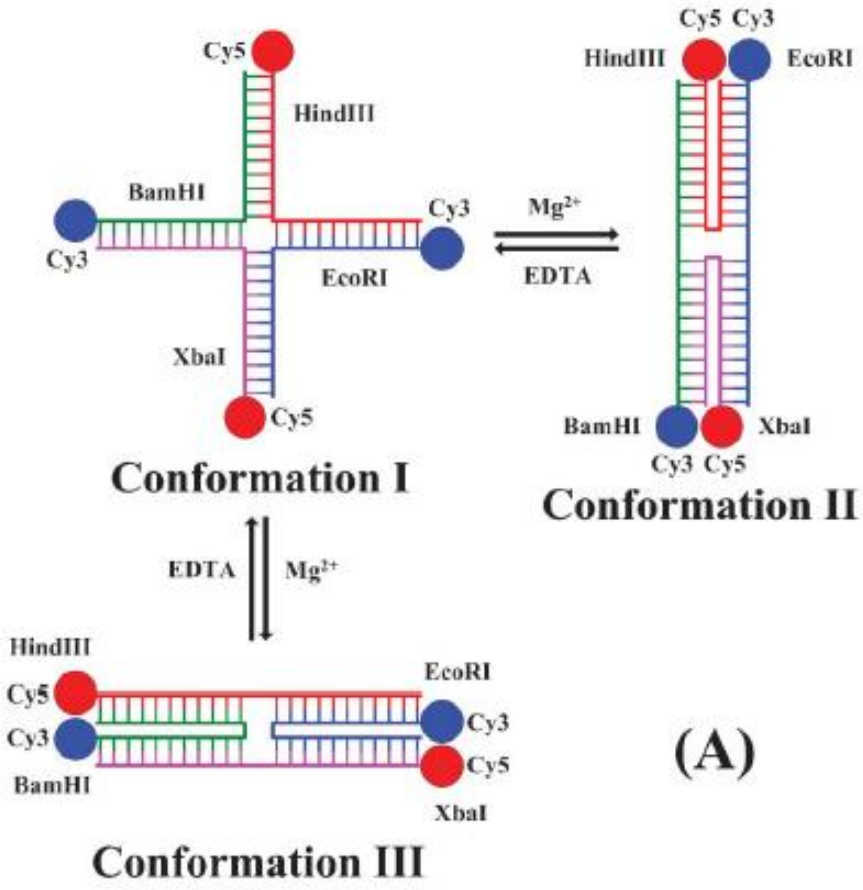

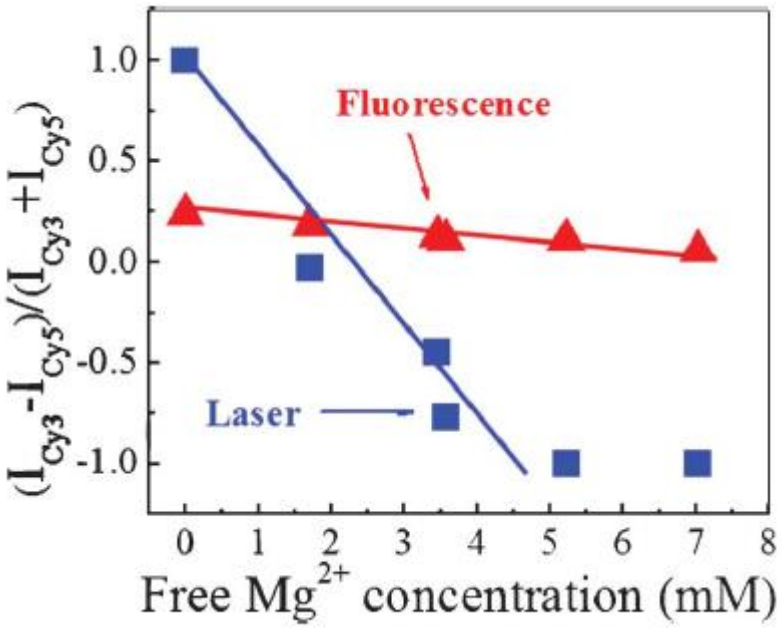

16 times more sensitivity experimentally demonstrated!

X. Zhang, W. Lee, and X. Fan, Lab Chip 12, 3673–3675 (2012)

Biosensing with Optofluidic Microlasers

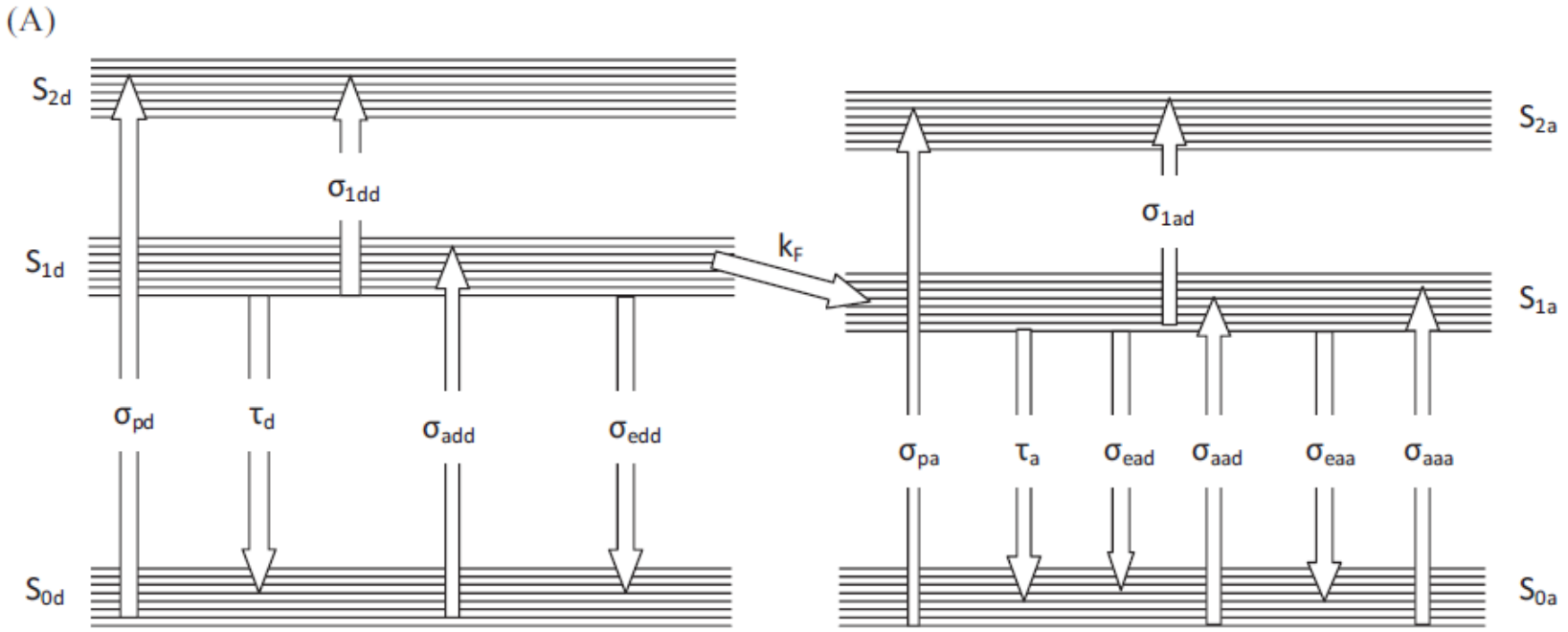

Biosensing with Optofluidic Microlasers

$$\frac{dn_d(t)}{dt} = I_p(t)\,\sigma_{pd}\left[N_d - n_d(t)\right] - \frac{\sigma_{edd}c}{\eta} n_d(t)\,q_d(t) + \frac{\sigma_{add}c}{\eta}\left[N_d - n_d(t)\right] q_d(t) - \frac{n_d(t)}{\tau_d} - k_F n_d(t)\,, \tag{1}$$

$$\frac{dq_d(t)}{dt} = \frac{Fc}{\eta}\left[\sigma_{edd} - \sigma_{1dd}\right] n_d(t)\,q_d(t) + \frac{Fc}{\eta V}\sigma_{edd} n_d(t) - \frac{Fc}{\eta}\sigma_{add}\left[N_d - n_d(t)\right] q_d(t) - \frac{q_d(t)}{\tau_{cd}} + \frac{Fc}{\eta}\sigma_{ead} n_a(t)\,q_d(t) - \frac{Fc}{\eta}\sigma_{1ad} n_a(t)\,q_d(t) - \frac{Fc}{\eta}\sigma_{aad}\left[N_a - n_a(t)\right] q_d(t)\,, \tag{2}$$

$$\frac{dn_a(t)}{dt} = I_p(t)\,\sigma_{pa}\left[N_a - n_a(t)\right] - \frac{\sigma_{ead}c}{\eta} n_a(t)\,q_d(t) - \frac{n_a(t)}{\tau_a} + \frac{\sigma_{aad}c}{\eta}\left[N_a - n_a(t)\right] q_d(t) - \frac{\sigma_{eaa}c}{\eta} n_a(t)\,q_a(t) + k_F n_d(t) + \frac{\sigma_{aaa}c}{\eta}\left[N_a - n_a(t)\right] q_a(t)\,, \tag{3}$$

$$\frac{dq_a(t)}{dt} = \frac{Fc}{\eta}\left[\sigma_{eaa} - \sigma_{1aa}\right] n_a(t)\,q_a(t) + \frac{Fc}{\eta V}\sigma_{eaa} n_a(t) - \frac{Fc}{\eta}\sigma_{aaa}\left[N_a - n_a(t)\right] q_a(t) - \frac{q_a(t)}{\tau_{ca}}\,. \tag{4}$$

Parameters

Constant	Description	Numeric Value
σ_{pd}	Donor absorption cross section at the pump wavelength	3.42×10^{-16} cm^2
σ_{pa}	Acceptor absorption cross section at the pump wavelength	0.05×10^{-16} cm^2
σ_{edd}	Donor stimulated emission cross section at λ_d	3.78×10^{-16} cm^2
σ_{eaa}	Acceptor stimulated emission cross section at λ_a	6.9×10^{-16} cm^2
σ_{ead}	Acceptor stimulated emission cross section at λ_d	0.036×10^{-16} cm^2
σ_{add}	Donor absorption cross section at λ_d	1.00×10^{-16} cm^2
σ_{1dd}	Excited state absorption cross section of donor molecules at λ_d	0.4×10^{-16} cm^2
σ_{1aa}	Excited state absorption cross section of acceptor molecules at λ_a	2.00×10^{-16} cm^2
σ_{1ad}	Excited state absorption cross section of acceptor molecules at λ_d	1.30×10^{-16} cm^2
σ_{aad}	Acceptor absorption cross section at λ_d	0.156×10^{-16} cm^2
σ_{aaa}	Acceptor absorption cross section at λ_a	1.00×10^{-16} cm^2
η	Refractive index of the medium	1.33
τ_d	Fluorescence lifetime of donor molecules	4 ns
τ_a	Fluorescence lifetime of acceptor molecules	3.3 ns
τ_{cd}	Fluorescence lifetime of cavity at λ_d	$Q_0\lambda_d/(2\pi c)$
τ_{ca}	Fluorescence lifetime of cavity at λ_a	$Q_0\lambda_a/(2\pi c)$
λ_d	Donor lasing wavelength	560 nm
λ_a	Acceptor lasing wavelength	655 nm
R_0	Förster radius	6.1 nm
Q_0	Empty cavity Q-factor	10^6
F	Fraction of mode volume occupied by the dye molecules	1
d	Depth of the electromagnetic mode	30 μm
w	Width of the electromagnetic mode	30 μm
l	Length of the electromagnetic mode	30 μm
V	Volume of the electromagnetic mode	dwl
Δt	Pump laser pulsewidth	5 ns
c	Speed of light in vacuum	3×10^{10} cm/s
h	Planck's constant	$6.62606957 \times 10^{-34}$ J $\cdot$ s

$$k_{F0} = \frac{1}{\tau_d}\left(\frac{R_0}{R}\right)^6$$

Results with a Non-Lasing Cavity (Q=1)

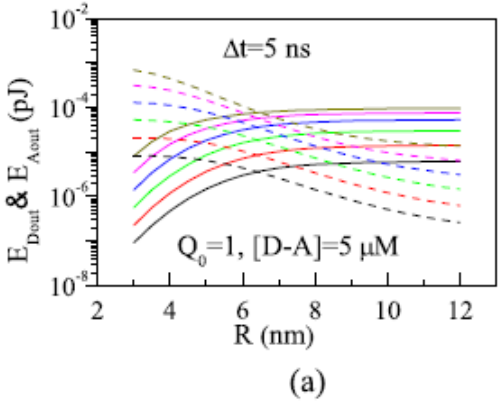

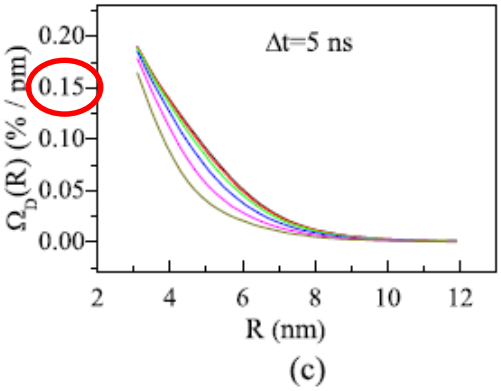

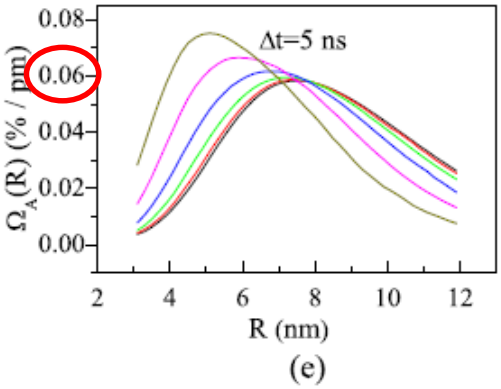

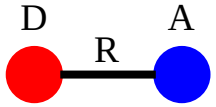

Non-Lasing Cavity, Q=1

$$Acceptor\ Sensitivity = \Omega_A = \left| 100 \frac{dE_{Aout}}{E_{Aout} dR} \right|$$

$$Donor\ Sensitivity = \Omega_D = \left| 100 \frac{dE_{Dout}}{E_{Dout} dR} \right|$$

Results with a Lasing Cavity (Q=10^6)

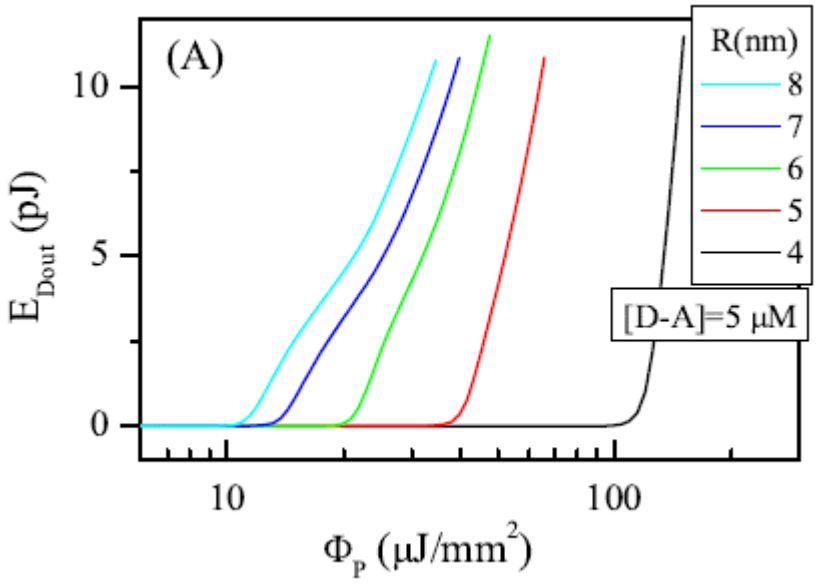

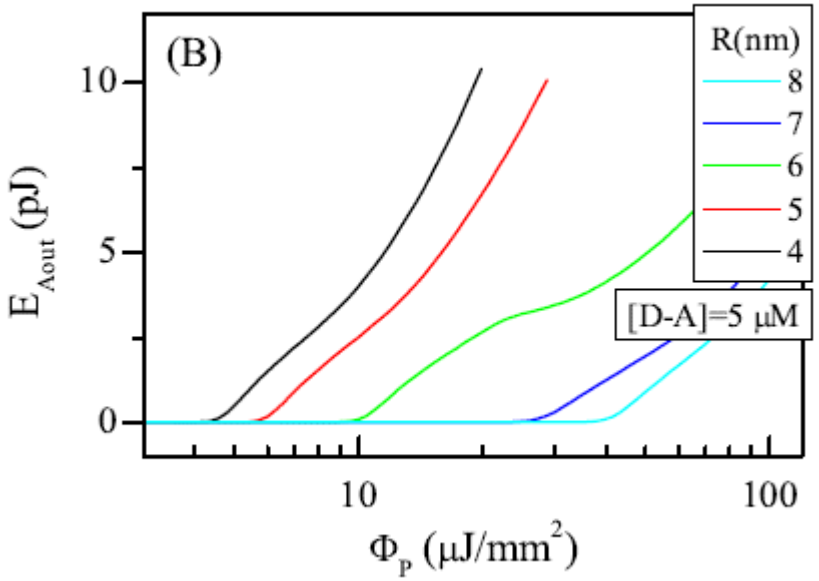

Results with a Lasing Cavity ($Q=10^6$)

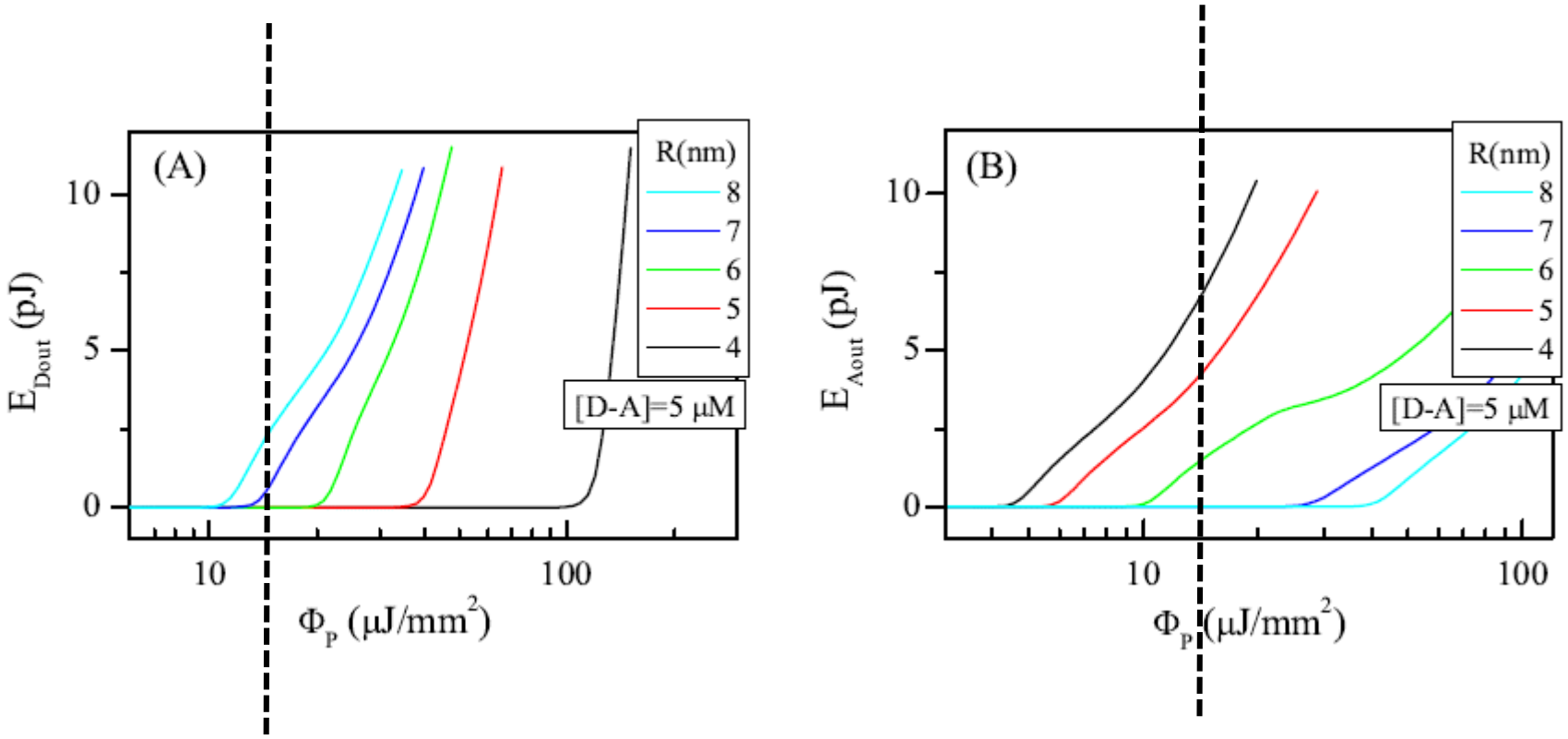

- Choose the pump intensity around acceptor lasing threshold
- Best results obtained around the Förster radius (6.1nm)

Results with a Lasing Cavity (Q=10^6)

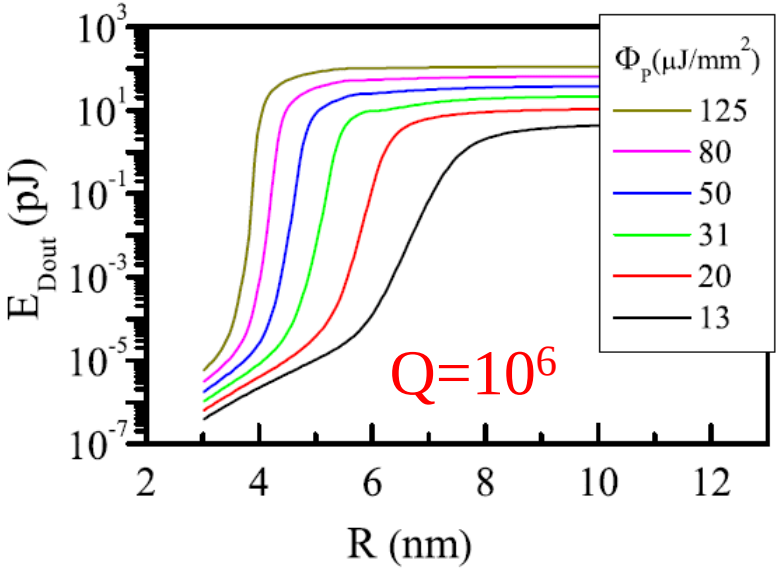

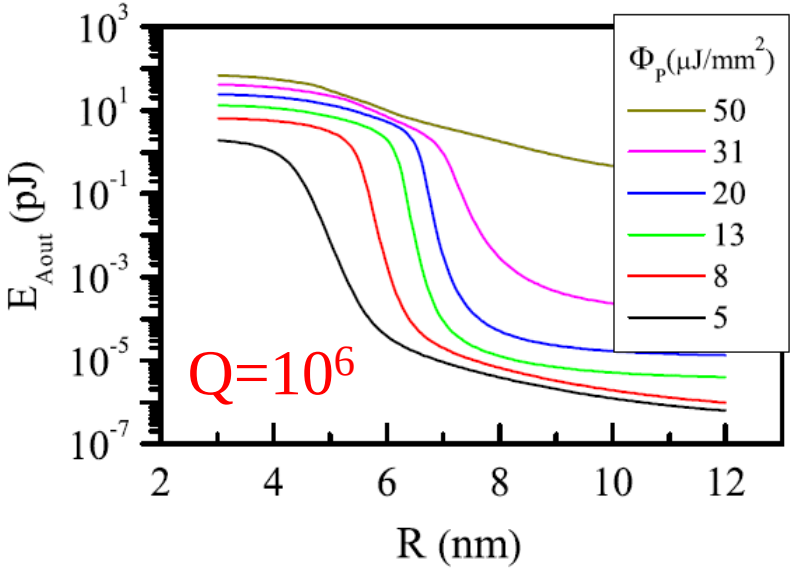

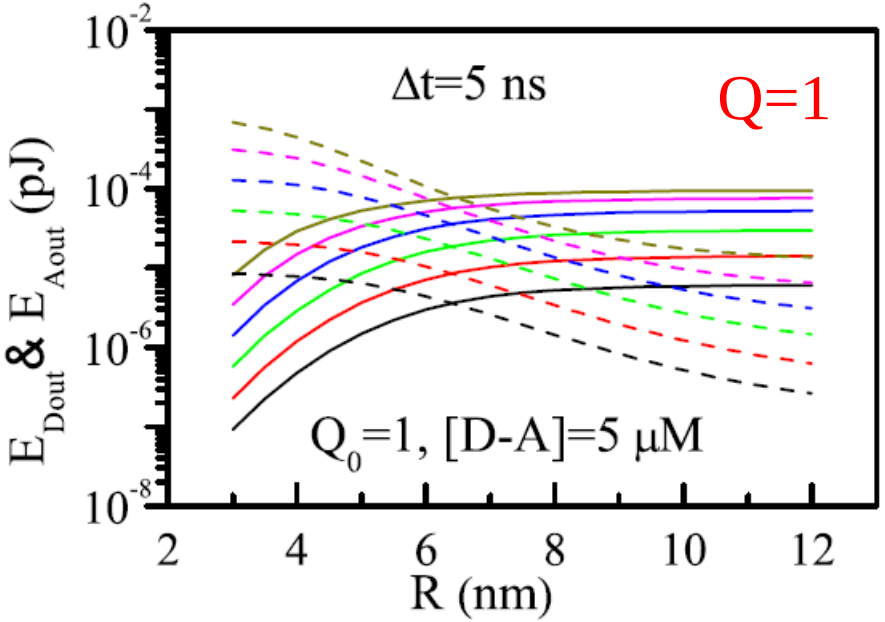

Results with a Lasing Cavity (Q=10^6)

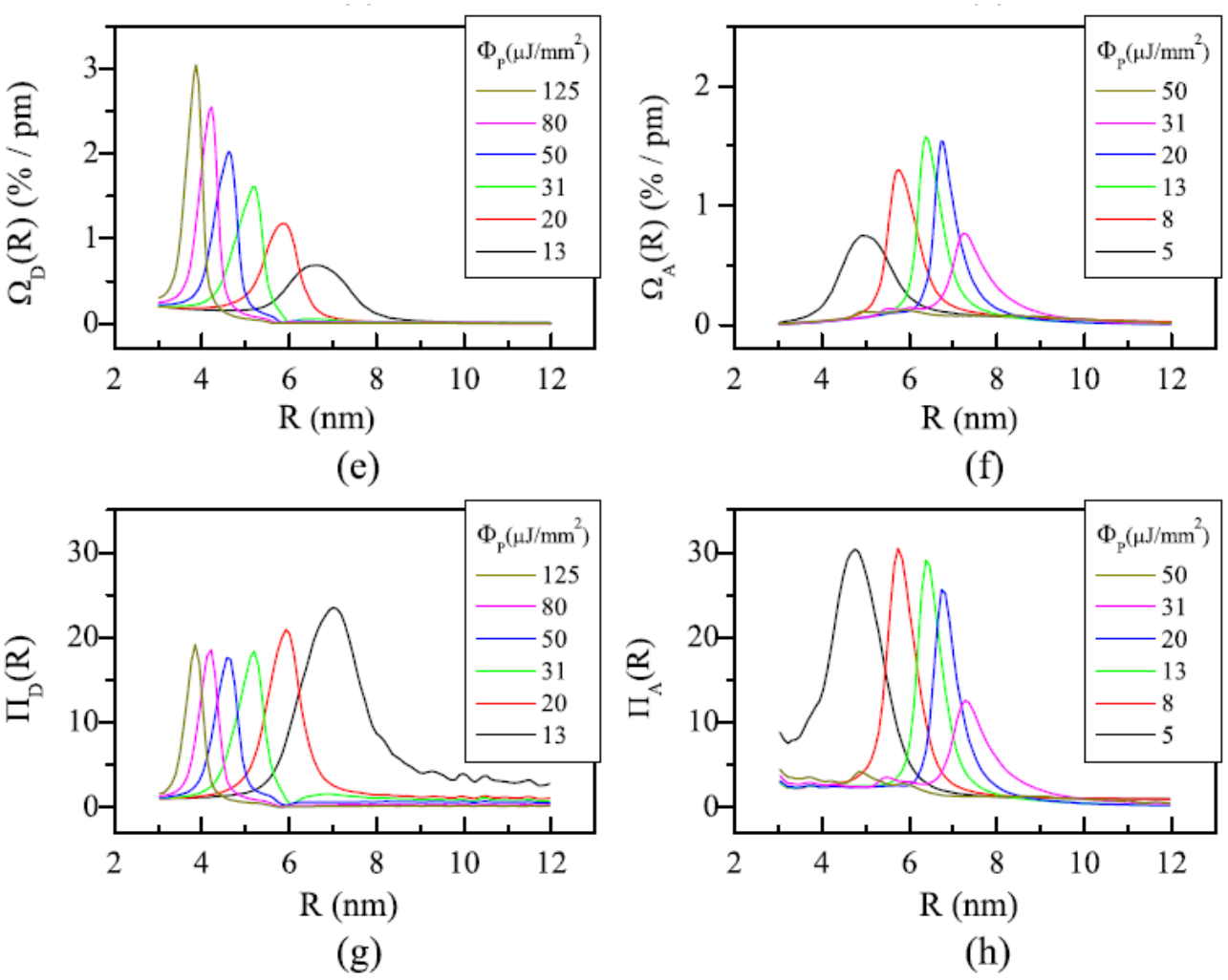

Sensitivity Enhancement Factors

$$\Pi_D(R) = \frac{\Omega_{D,lasing}(R)}{\Omega_{D,fluorescence}(R)}$$

$$\Pi_A(R) = \frac{\Omega_{A,lasing}(R)}{\Omega_{A,fluorescence}(R)}$$

Results with a Lasing Cavity (Q=10^6)

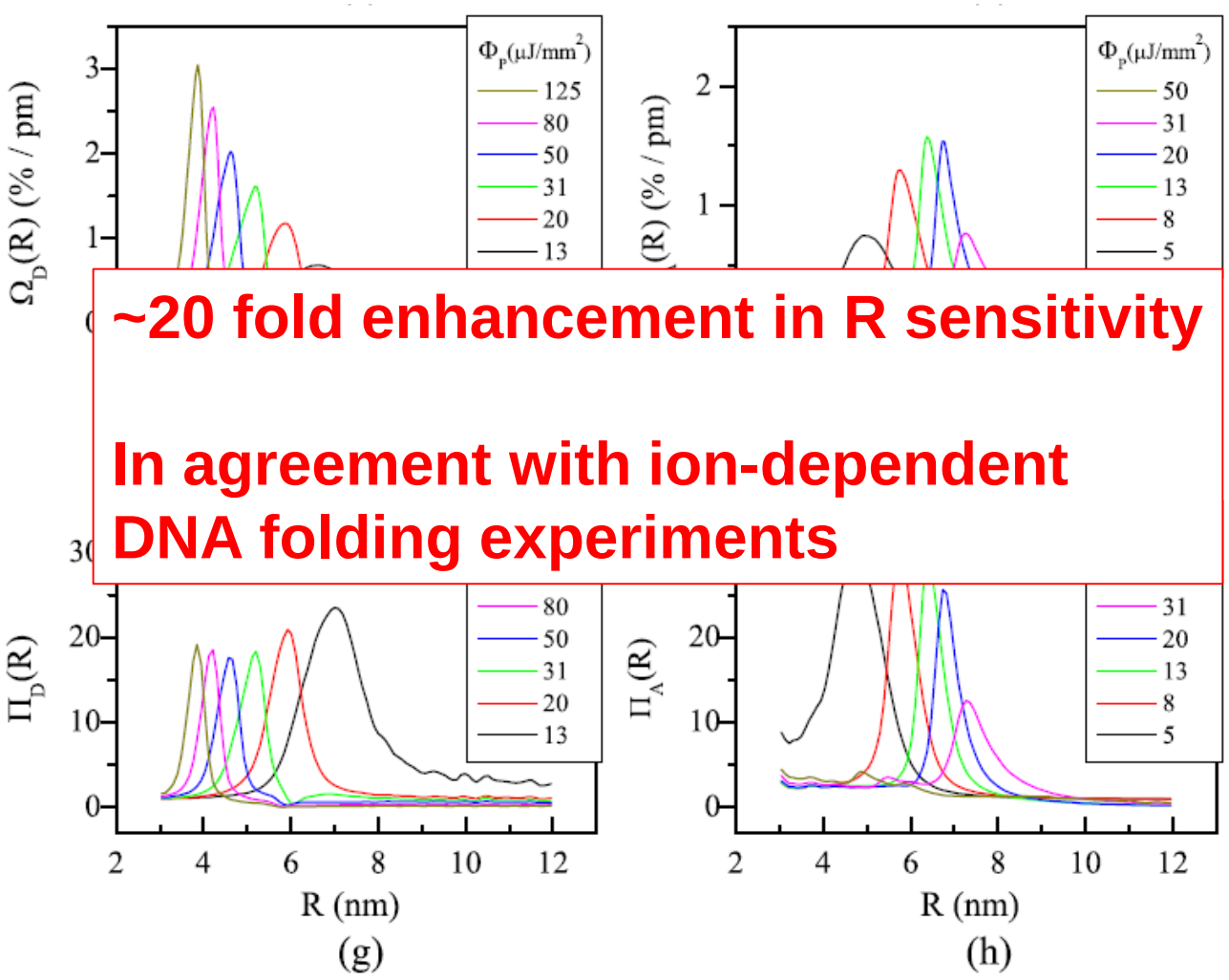

~20 fold enhancement in R sensitivity

In agreement with ion-dependent DNA folding experiments

Sensitivity Enhancement Factors

$$\Pi_D(R) = \frac{\Omega_{D,lasing}(R)}{\Omega_{D,fluorescence}(R)}$$

$$\Pi_A(R) = \frac{\Omega_{A,lasing}(R)}{\Omega_{A,fluorescence}(R)}$$

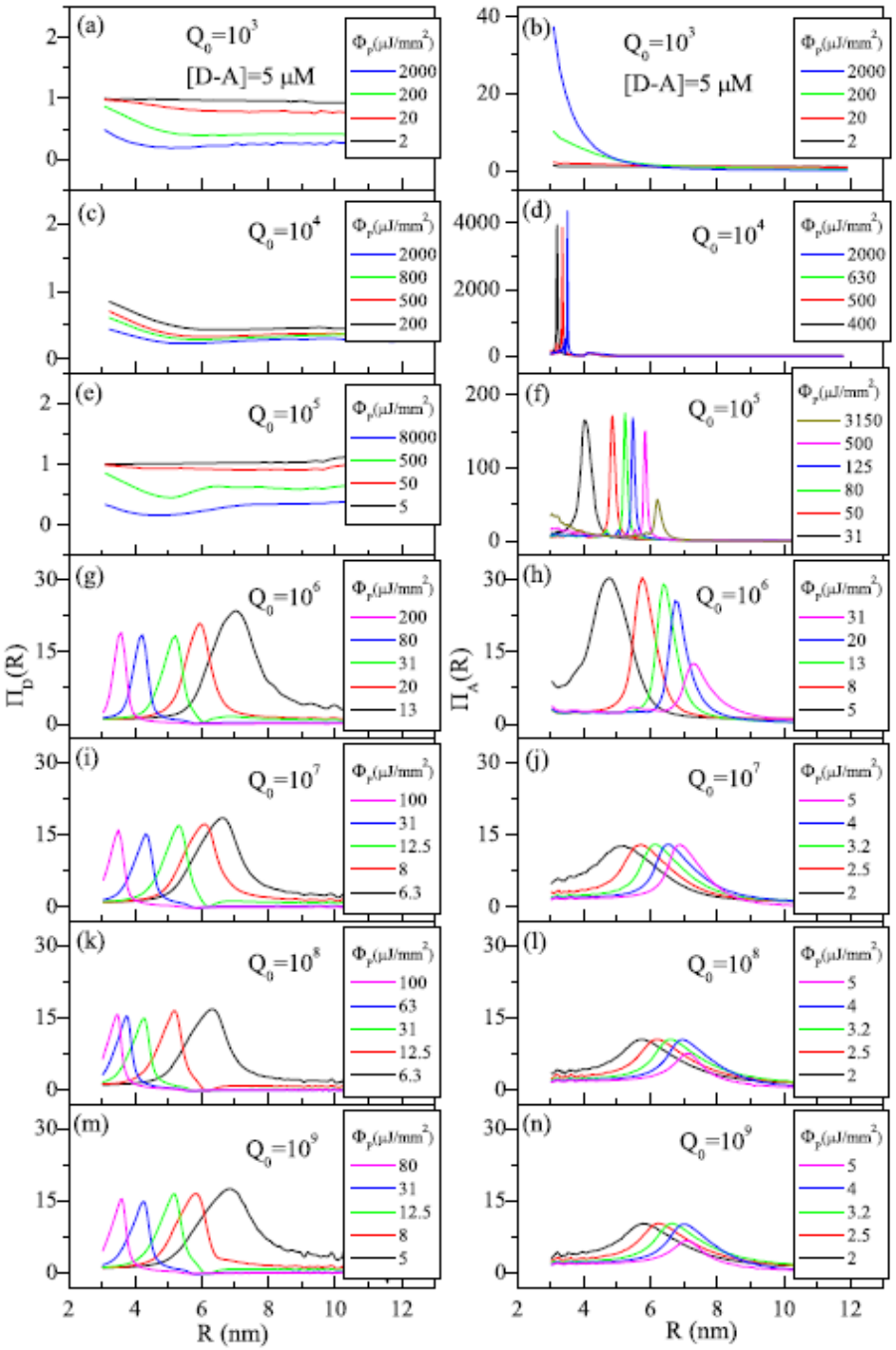

Enhancement does not increase with Q-factor

Best performance is observed for $Q=10^4$-10^5 where donor lasing is missing

Enhancement in Concentration Sensitivities

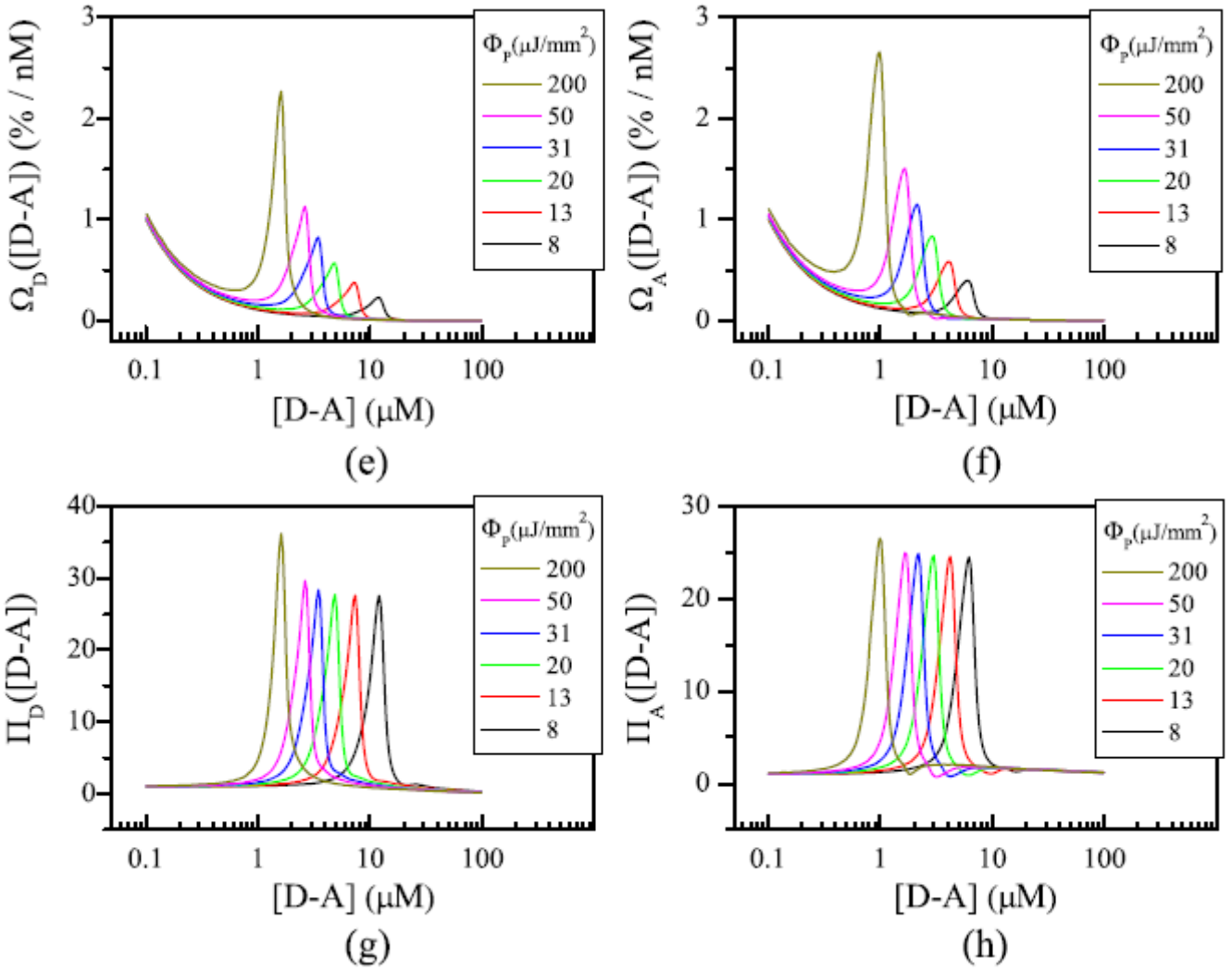

Enhancement in Concentration Sensitivities

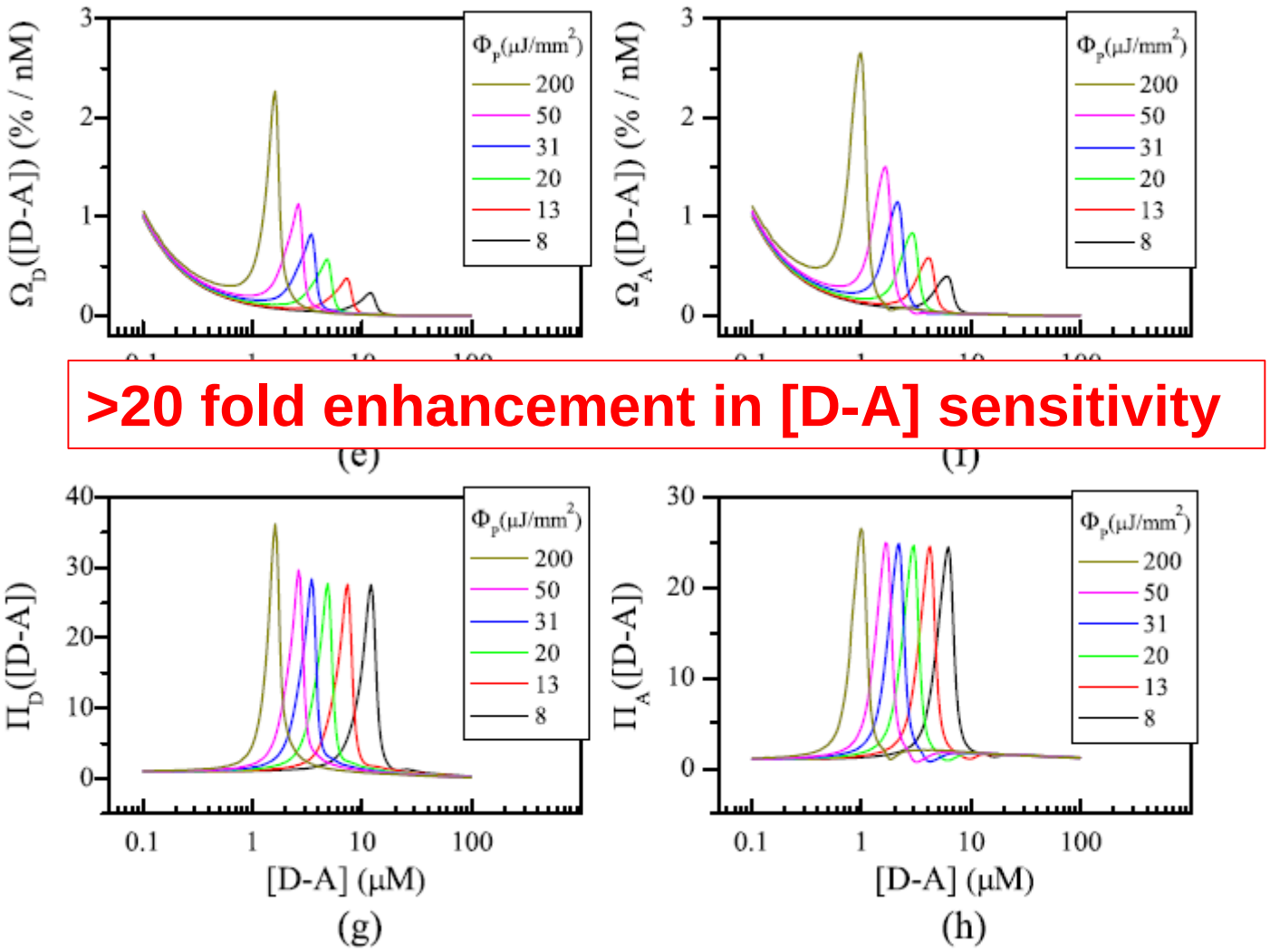

>20 fold enhancement in [D-A] sensitivity

Conclusions 1

- Biochemical sensors based on FRET lasing from linked donor–acceptor complexes can bring about more than 20-fold enhancement of detection sensitivity of conformation changes of the complex for linker lengths comparable to the Förster Radius of the donor–acceptor pair.

- Our analysis has revealed that cavities with Q-factors between 10^4–10^6 enable optimal sensing performance.

- More than 1% change can be observed in donor or acceptor emission intensities for 1 nM change in dye-pair concentration of approximately1 μM.

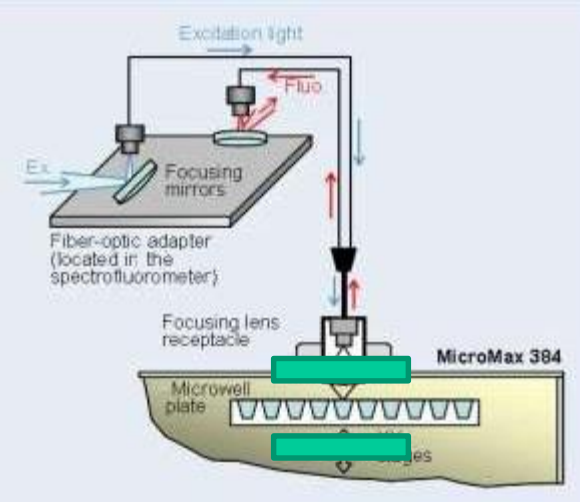

Can we develop a lasing based microplate reader?

M. Aas, Q. Chen, A. Jonáš, A. Kiraz, and X. Fan, IEEE J. Sel. Top. Quan. (2016)

OPTOFLUIDIC LASING WITH AQUEOUS QUANTUM DOTS

Optofluidic Ring Resonator

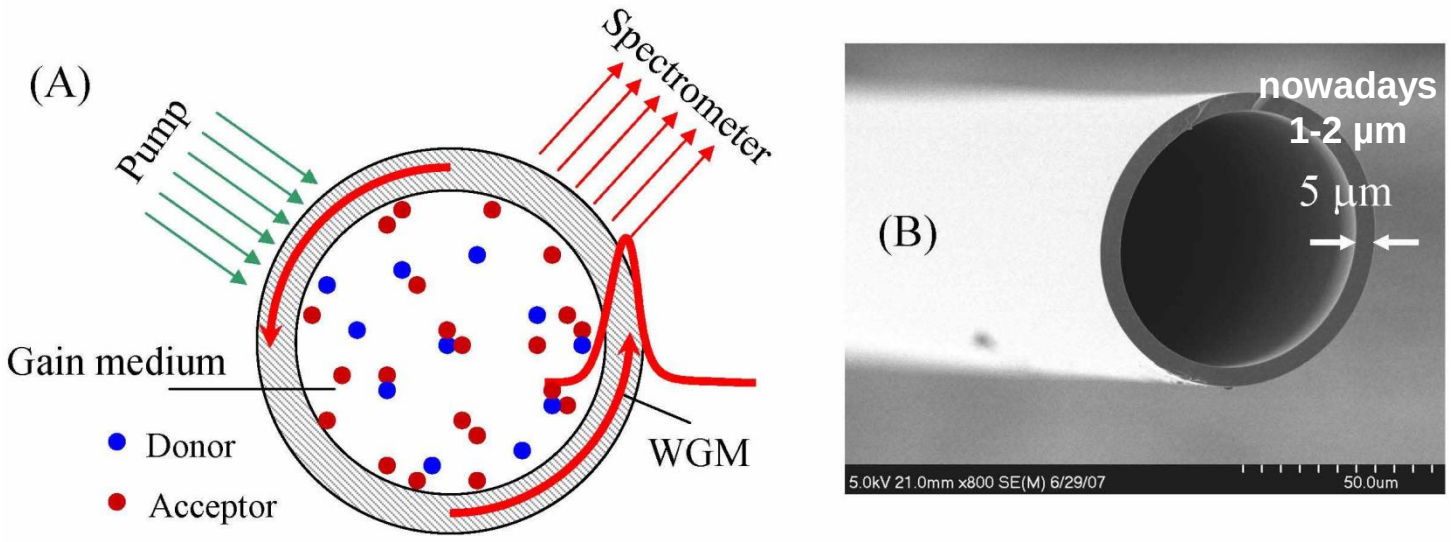

Y. Sun and X. Fan, Angew. Chem. Int. Ed. (2012)
X. Fan, S.-H. Yun, Nature Methods (2014)
S.I. Shopova et al. Opt. Express (2007)

Two step fabrication:

- HF etching
- Pulling under CO_2 laser irradiation

$Q>10^6$

V is large

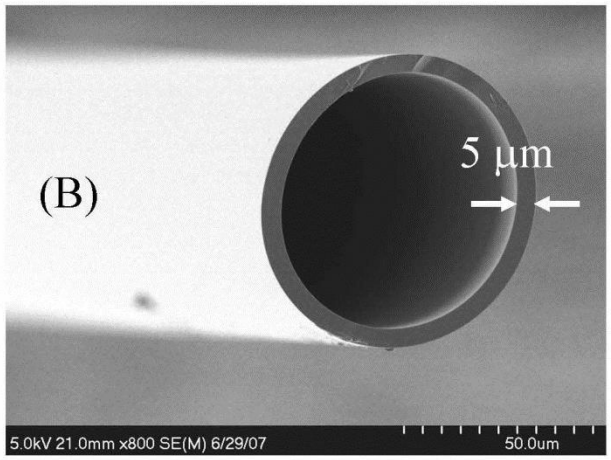

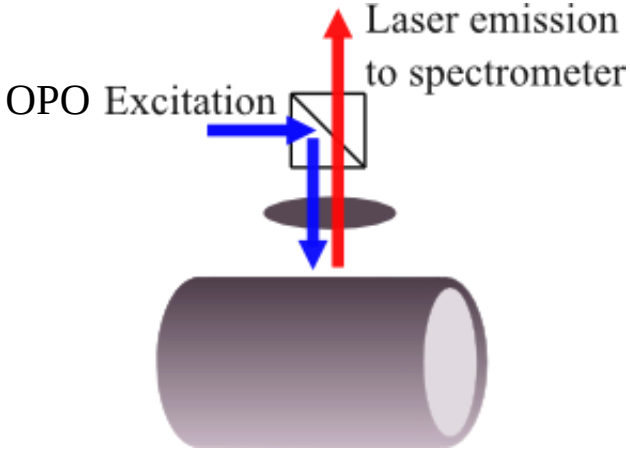

n_{fused_silica}=1.46

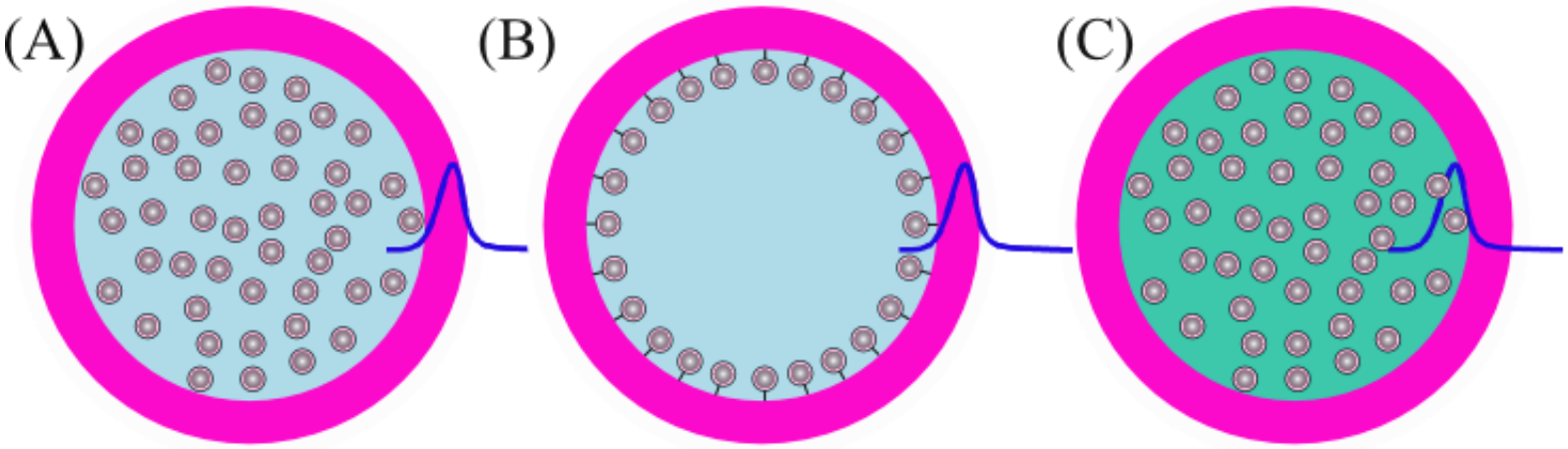

Aqueous QDs in solution

n_{water}=1.33

Surface immobilized aqueous QDs

n_{water}=1.33

QDs in toluene

$n_{toluene}$=1.49

CdSeS/ZnS alloyed quantum dots fluorescence λ_{em} 575 nm and λ_{em} 630 nm, 6 nm diameter, 1 mg/mL in toluene

CdSeS/ZnS alloyed quantum dots, 6 nm diameter, 1 mg/mL in water

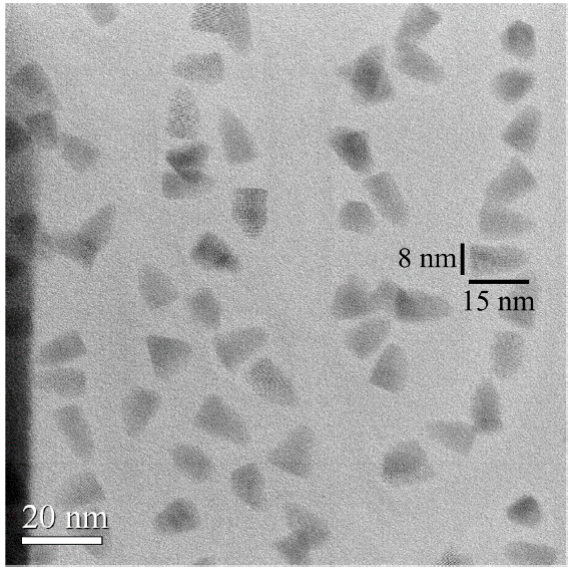

Qdot ® 655, CdSe/ZnS quantum dots, 8 x 15 nm, in water

CdSeS/ZnS alloyed quantum dots fluorescence λ_{em} 575 nm and λ_{em} 630 nm, 6 nm diameter, 1 mg/mL in toluene

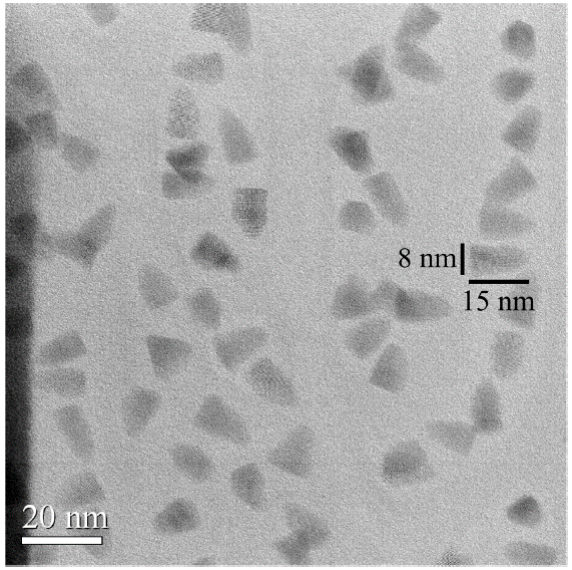

~~CdSeS/ZnS alloyed quantum dots, 6 nm diameter, 1 mg/mL in water~~

Qdot ® 655, CdSe/ZnS quantum dots, 8 x 15 nm, in water

Alloyed QDs in Toluene

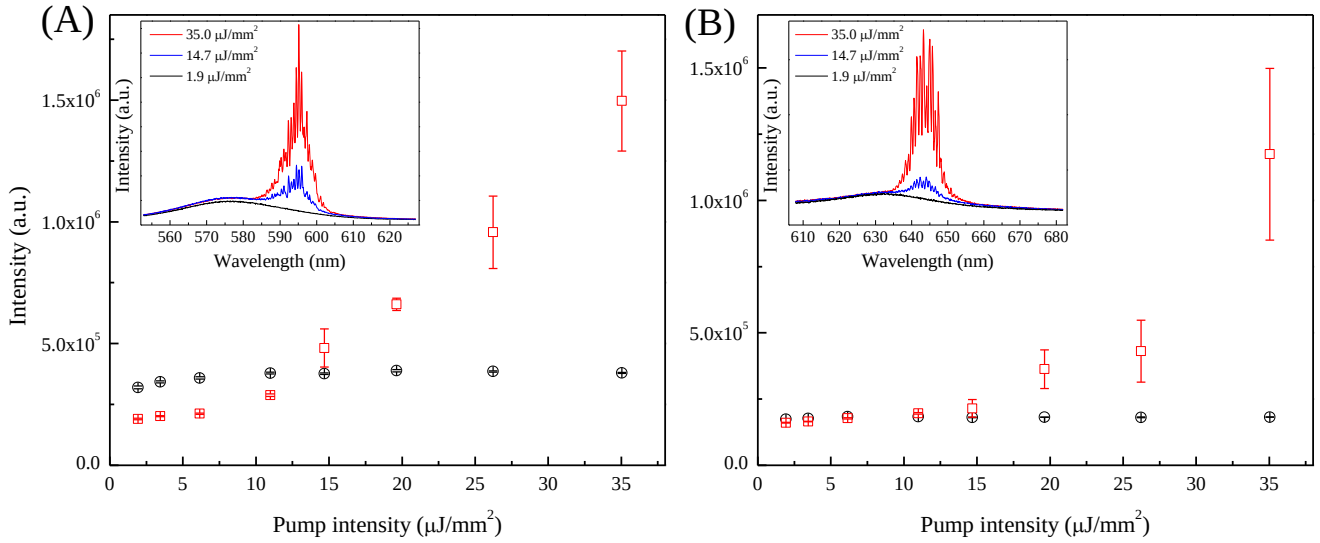

QD concentration 2 μM

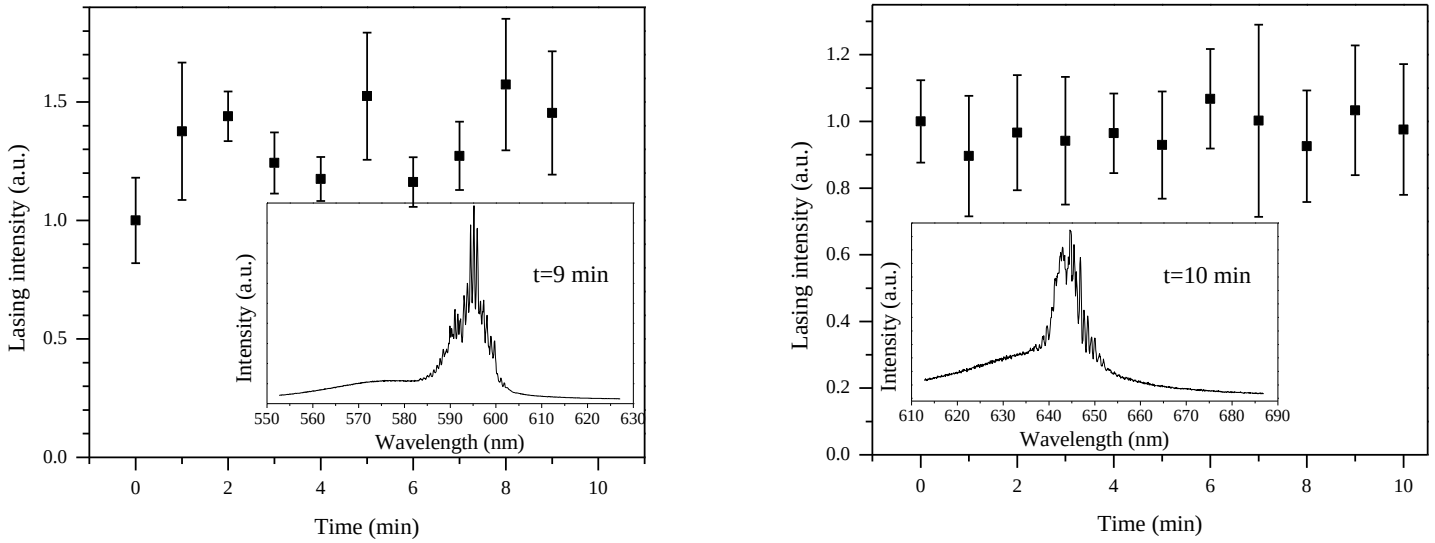

Qdot ® 655 in Water

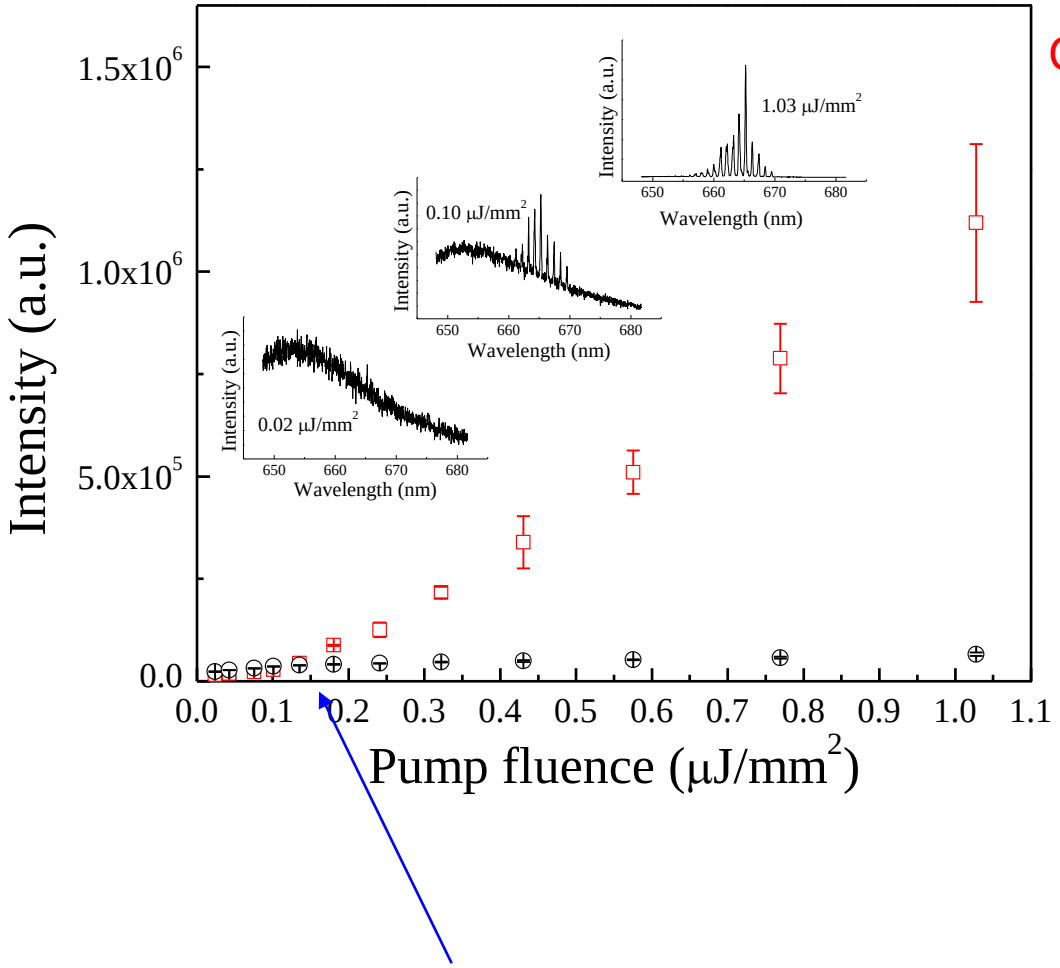

QD concentration 2 μM

Ultralow threshold: 0.1 μJ/mm^2

Large Absorption Cross-Section of Rod-Like QDs

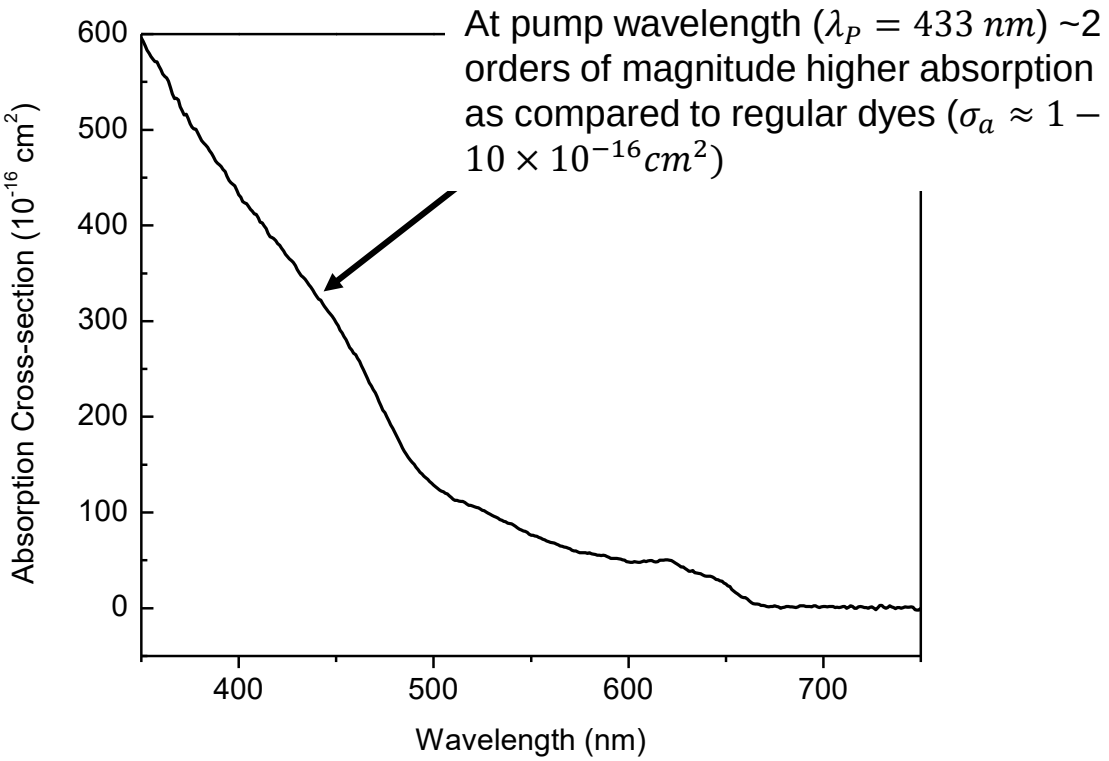

A large absorption cross section is an intrinsic property of the QDs related to their size, which is much larger than the size of an organic dye molecule.

Our QDs have a rod-like geometry that further increases the absorption due to the behavior of their shell as an efficient antenna.

Qdot ® 655 in Water

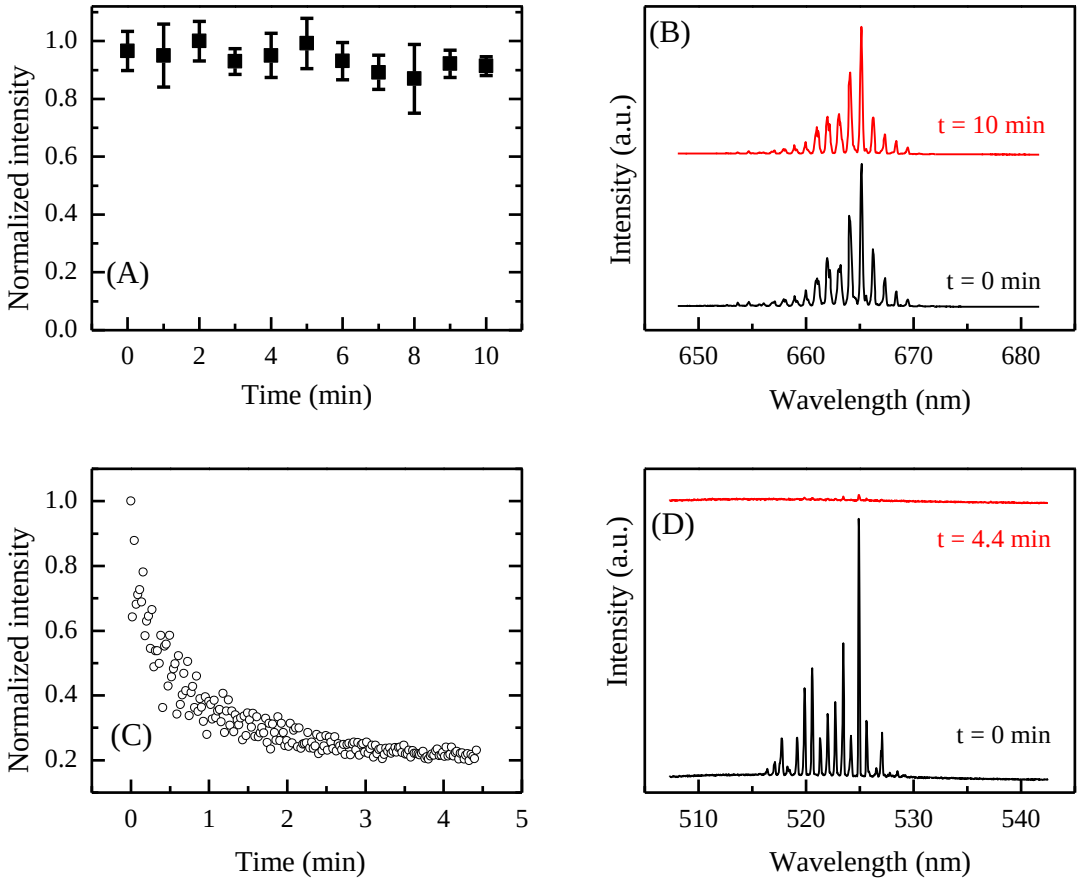

Multiexcitons in QDs

V.I. Klimov et al.

$\langle N \rangle$ Average number of excitons in the QD

$P(N) = \langle N \rangle^N \frac{e^{-\langle N \rangle}}{N!}$ Probability of having N excitons in the QD. Poisson distribution (*Due to state-filling effect).*

State filling requires biexciton emission from the S band when N>2

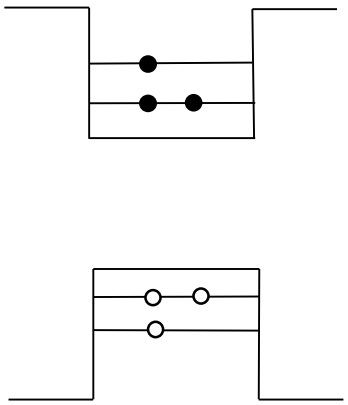

Biexciton-exciton cascade

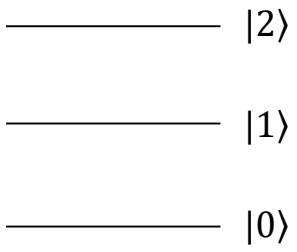

Lasing Threshold Condition

V.I. Klimov et al.

$\langle N \rangle$ Average number of excitons in the QD

$P(N) = \langle N \rangle^N \frac{e^{-\langle N \rangle}}{N!}$ Probability of having N excitons in the QD. Poisson distribution.

$$\sigma_{e,X}(\lambda_L)[n_T P(1)] + \sigma_{e,XX}(\lambda_L)[n_T P(2)] + \sigma_{e,XX}(\lambda_L)$$
$$[n_T P(3)]... = \sigma_a(\lambda_L)[n_T P(0)] + \frac{\sigma_a(\lambda_L)}{2}[n_T P(1)]$$
$$+ \frac{2\pi m}{\lambda_L \eta Q_0} \qquad (1)$$

Lasing Threshold Condition

V.I. Klimov et al.

$\langle N \rangle$ Average number of excitons in the QD

$P(N) = \langle N \rangle^N \frac{e^{-\langle N \rangle}}{N!}$ Probability of having N excitons in the QD. Poisson distribution.

$$1 - P(0) - \frac{P(1)}{2} = \frac{\sigma_a(\lambda_L)}{\sigma_{e,XX}(\lambda_L)} P(0) + \frac{\sigma_a(\lambda_L)}{2\sigma_{e,XX}(\lambda_L)} P(1) + \frac{2\pi m}{\sigma_{e,XX}(\lambda_L) n_T \lambda_L \eta Q_0}$$

Lasing Threshold Condition

V.I. Klimov et al.

$\langle N \rangle$ Average number of excitons in the QD

$P(N) = \langle N \rangle^N \frac{e^{-\langle N \rangle}}{N!}$ Probability of having N excitons in the QD. Poisson distribution.

$$1 - P(0) - \frac{P(1)}{2} = \frac{\sigma_a(\lambda_L)}{\sigma_{e,XX}(\lambda_L)} P(0) + \frac{\sigma_a(\lambda_L)}{2\sigma_{e,XX}(\lambda_L)} P(1) + \frac{2\pi m}{\sigma_{e,XX}(\lambda_L) n_T \lambda_L \eta Q_0}$$

$$\sigma_e(\lambda_L) = \frac{\lambda_L{}^4 E(\lambda_L)}{8\pi c n_L{}^2 \tau_F}$$

$$\sigma_{e,XX}(\lambda_L) = 2\sigma_{e,X}(\lambda_L)$$

We find $\langle N \rangle = 4.1$ at threshold.

This corresponds to $\Phi_{th} = 0.54\ \mu J/mm^2$.

Close to the experimental value $\Phi_{th} = 0.1\ \mu J/mm^2$.

Lasing Threshold Condition

V.I. Klimov et al.

$\langle N \rangle$ Average number of excitons in the QD

$P(N) = \langle N \rangle^N \frac{e^{-\langle N \rangle}}{N!}$ Probability of having N excitons in the QD. Poisson distribution.

$$1 - P(0) - \frac{P(1)}{2} = \frac{\sigma_a(\lambda_L)}{\sigma_{e,XX}(\lambda_L)} P(0) + \frac{\sigma_a(\lambda_L)}{2\sigma_{e,XX}(\lambda_L)} P(1) + \frac{2\pi m}{\sigma_{e,XX}(\lambda_L) n_T \lambda_L \eta Q_0}$$

Assume very large $\langle N \rangle$, $P(0) = P(1) = 0$.

$$n_{T\text{-min}} = \frac{2\pi m}{\sigma_{e,XX}(\lambda_L)\lambda_L \eta Q_0}$$

We obtain $n_{T-min} = 0.65\ \mu M$.

Surface Immobilized QDs

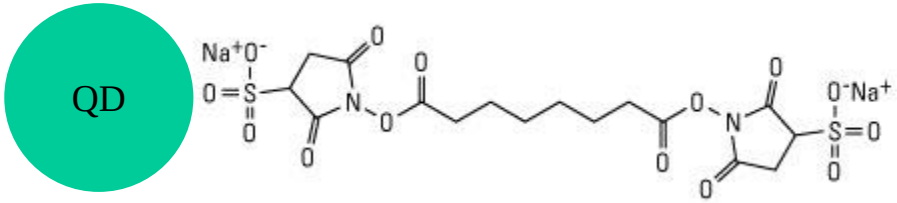

Amine groups on silanized silica surface

BS3
Bis(sulfosuccinimidyl) suberate
MW 572.43
Spacer Arm 11.4 Å

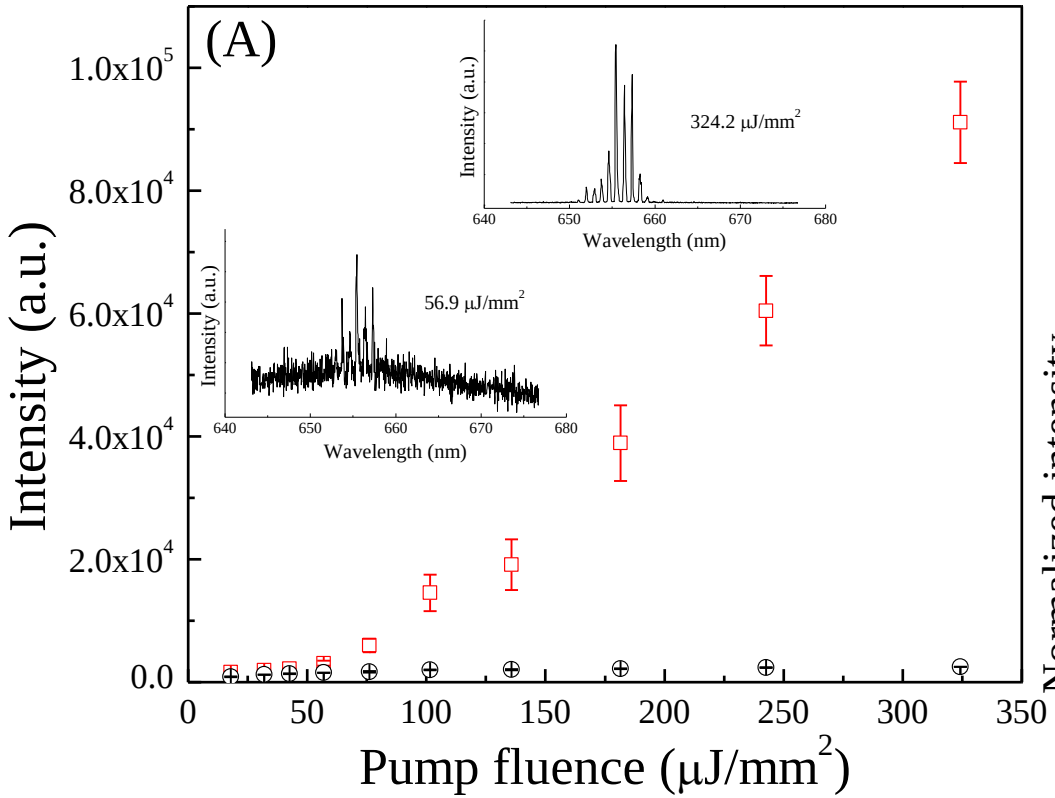

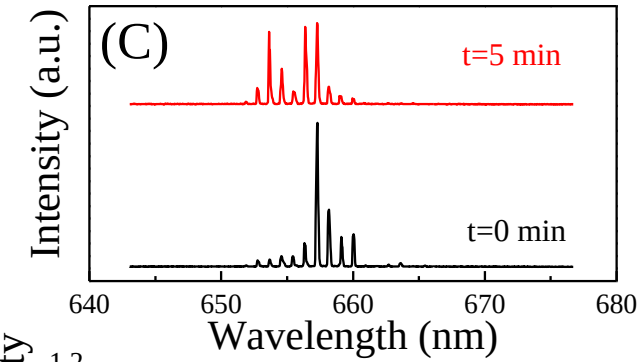

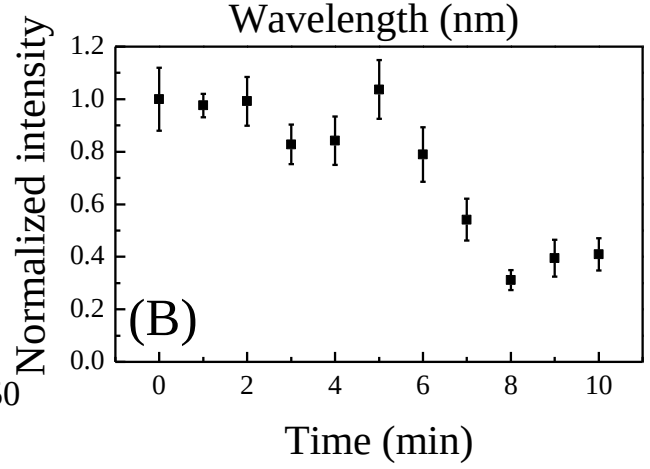

Surface Immobilized QDs

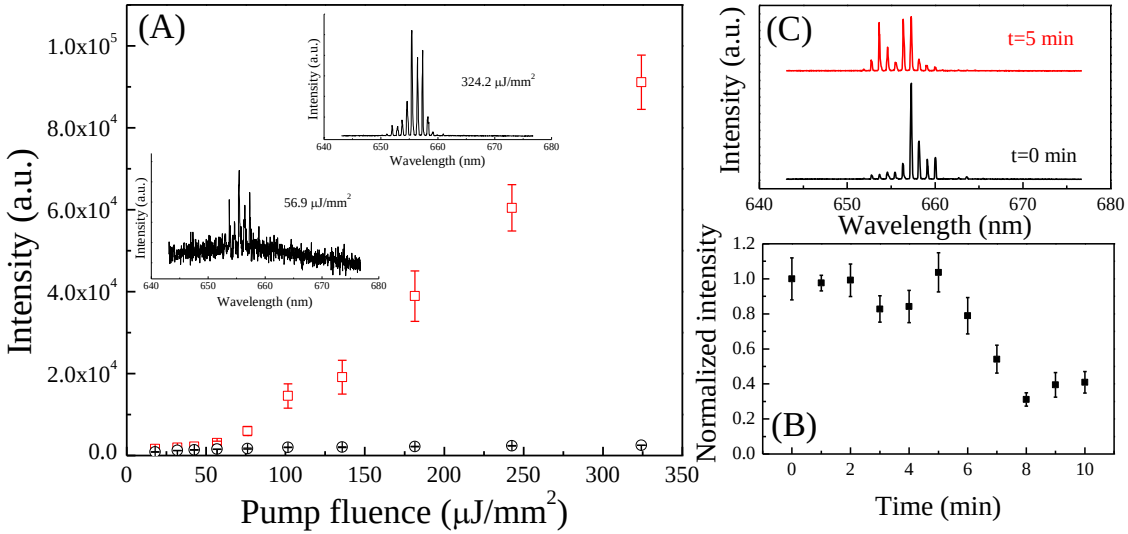

Very high pumping regime: $0.52\ \mu M < n_{T\_eff} < 2\mu M$.

Implies 0.37 % – 1.44 % surface coverage

Conclusions 2

- By combining the excellent fluorescent properties of the state-of-the-art core/shell QDs with the unique properties of the OFRR as an optical cavity, we demonstrated optofluidic QD lasing using aqueous solutions.

- Thanks to the high absorption cross section of QDs and excellent Q-factor of the WGMs in the OFRR, lasing was achieved at ultralow pump intensities when a bulk QD solution was used as the laser gain medium.

- In both bulk and surface immbilized cases stable QD lasing was achieved for durations longer than 5 min, sufficient for many biosensing applications.

- Second lasing demonstration with aqueous QDs (J. Schäfer et al., *Quantum dot microdrop laser*, Nano Lett. **8**, 1709−1712 (2998)).

A. Kiraz, Q. Chen, and X. Fan, ACS Photonics (2015)

OPTOFLUIDIC FRET LASING WITH AQUEOUS QUANTUM DOTS AS DONORS

QD-Cy5 Dye FRET Pairs

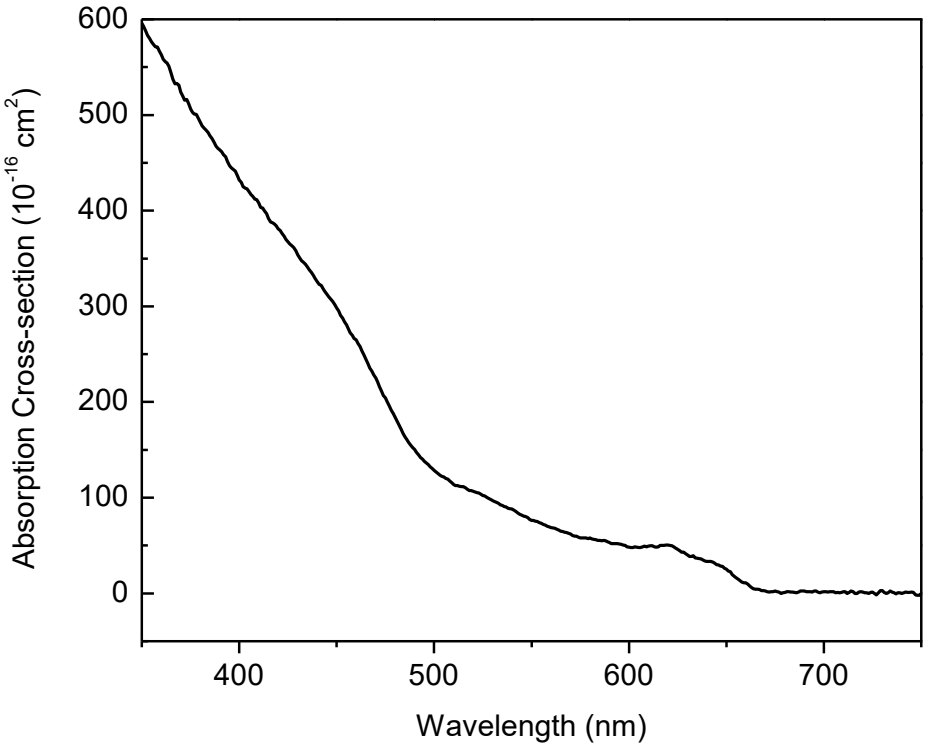

QDs are suitable as donors due to their broad absorption bands.

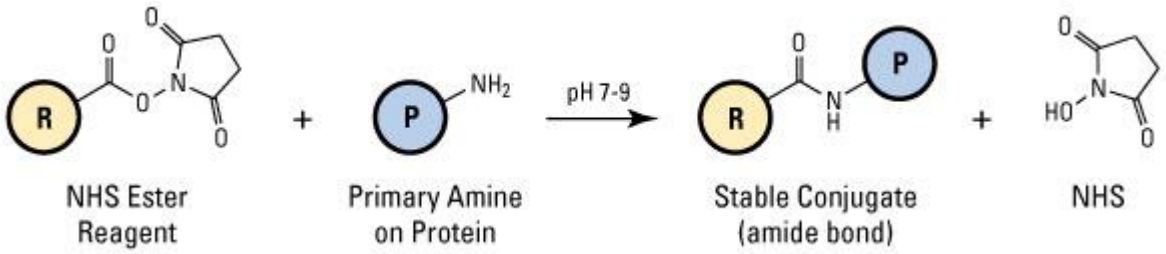

Cy5 NHS Ester was linked to Qdot 655 having amine group on it. (incubation and column filtering was used)

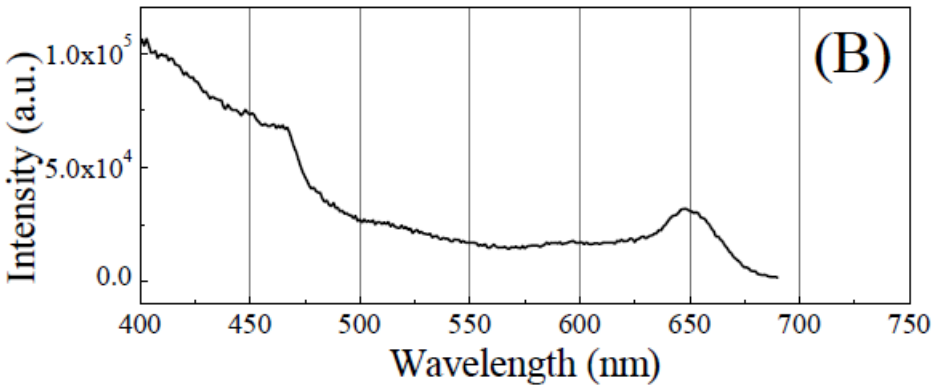

PLE

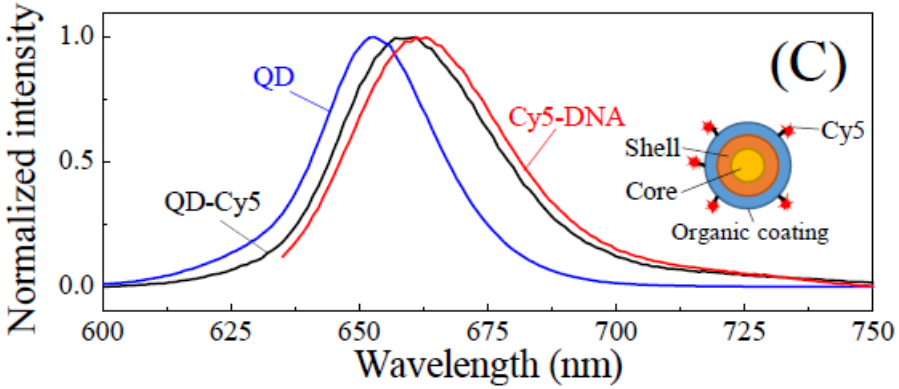

Emission implies 100% FRET efficiency

Cy5 concentration always 29 µM

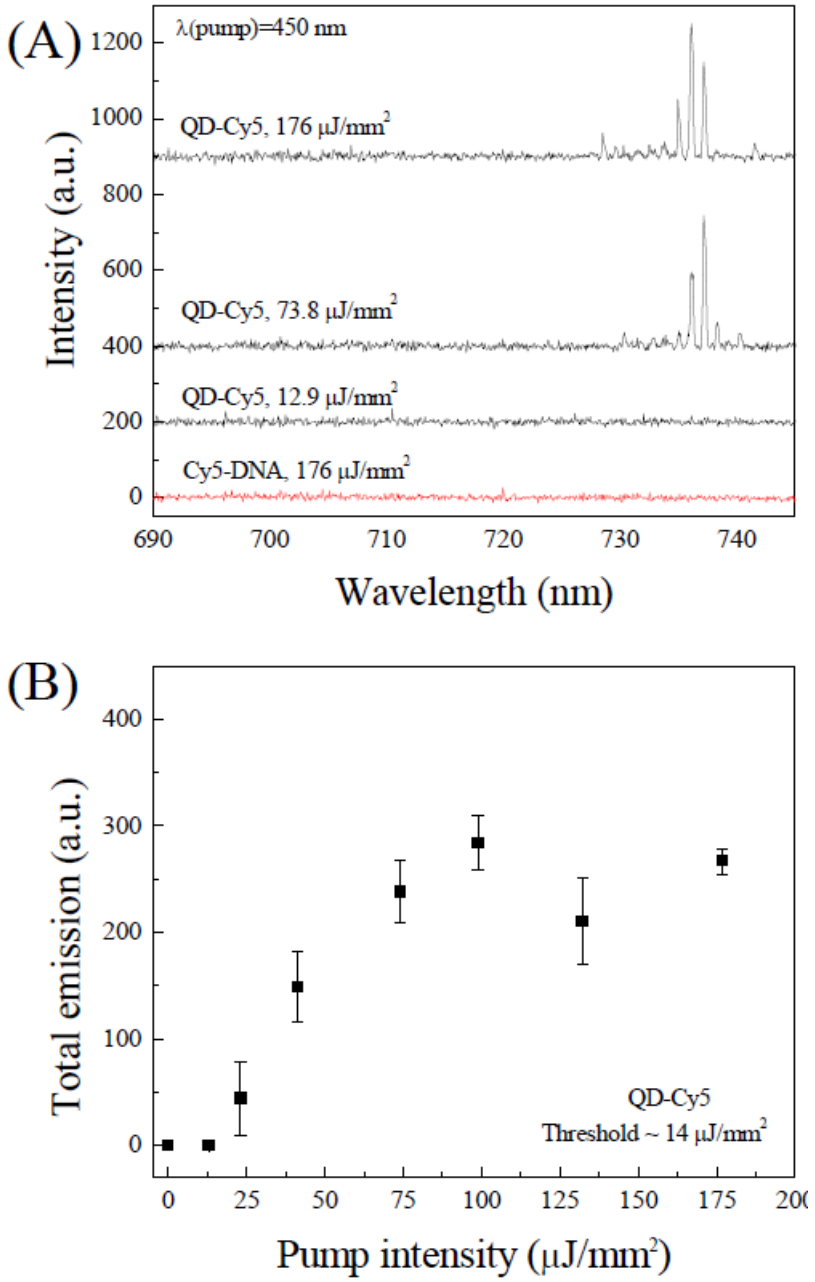

FRET Lasing Stability Analysis

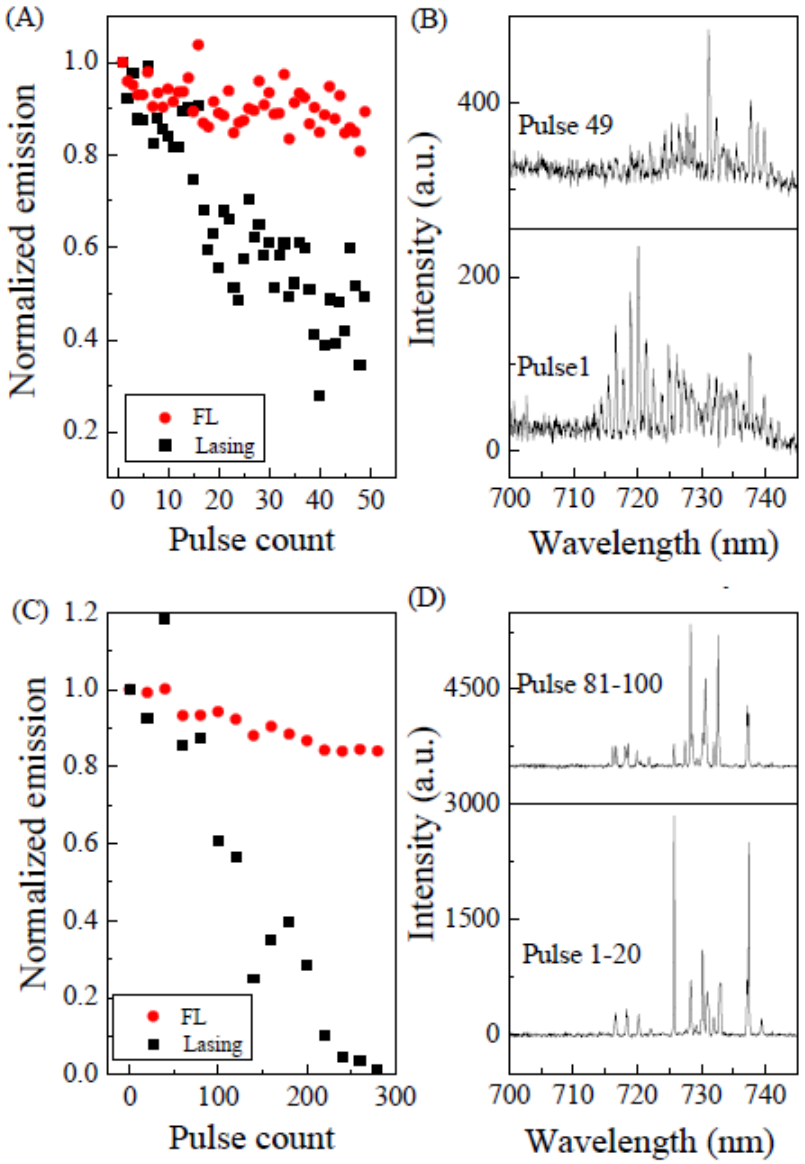

Photobleaching of Cy5

Rate Equations

$$\frac{dn_d}{dt} = I_p \sigma_{d,a}(N_d - n_d) - \frac{n_d}{\tau_d} - k_F n_d \qquad (1)$$

$$\frac{dn_a}{dt} = k_F n_d - \frac{n_a}{\tau_a} \qquad (2)$$

$$\frac{dq_a}{dt} = \frac{c}{m}\sigma_{a,e}(\lambda_L) n_a - \frac{c}{m}\sigma_{a,a}(\lambda_L)(N_a - n_a) - \frac{q_a}{\tau_{cavity}} \qquad (3)$$

Steady State Solution

$$n_d = \frac{I_p \sigma_{d,a}}{I_p \sigma_{d,a} + 1/\tau_d + k_F} N_d \qquad (4)$$

$$n_a = \tau_a k_F n_d \quad (5)$$

$$\sigma_{a,e}(\lambda_L) n_a - \sigma_{a,a}(\lambda_L)(N_a - n_a) - \frac{2\pi m}{Q_0 \lambda_L} = 0 \quad (6)$$

$$\gamma_{th} = \frac{n_{a,th}}{N_a} \approx \frac{\sigma_{a,a}(\lambda_L) N_a + 2\pi m/(Q_o \lambda_L)}{N_a \sigma_{a,e}(\lambda_L)}. \qquad (7)$$

We find $n_{a,th} = 0.41\ \mu M$ and $\gamma_{th} = 1.4\%$.

Pure DNA-Cy5 Experiments

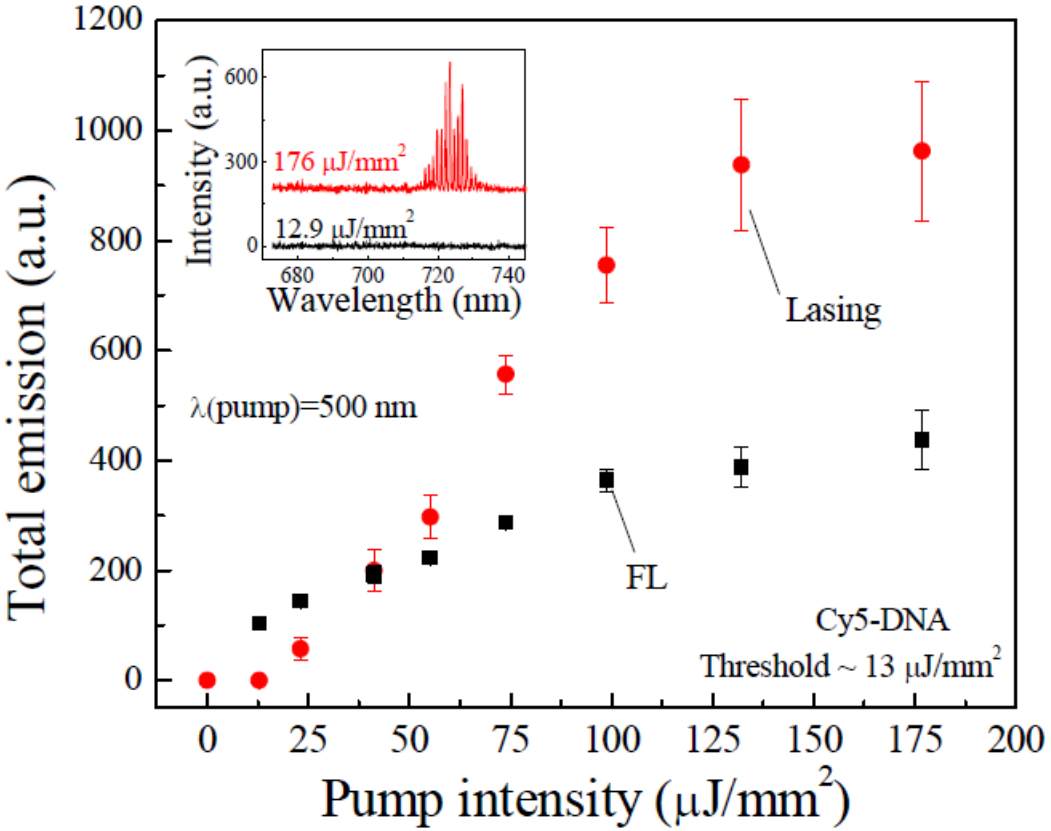

$$n_a = \frac{I_p \sigma_{a,a}(500nm)}{I_p \sigma_{a,a}(500nm) + 1/\tau_a} N_a$$

Experiments with pure DNA-Cy5 conjugates reveal:

$\gamma_{th} = 2\%$ with 29 μM concentration.

Good agreeement with $\gamma_{th} = 1.4\%$ predicted from the rate equation model.

Problem with Auger Recombination

At high pump powers τ_d decreases.

This implies n_d cannot be increased very well.

Hence, the required population invesion for the acceptor may not be achieved

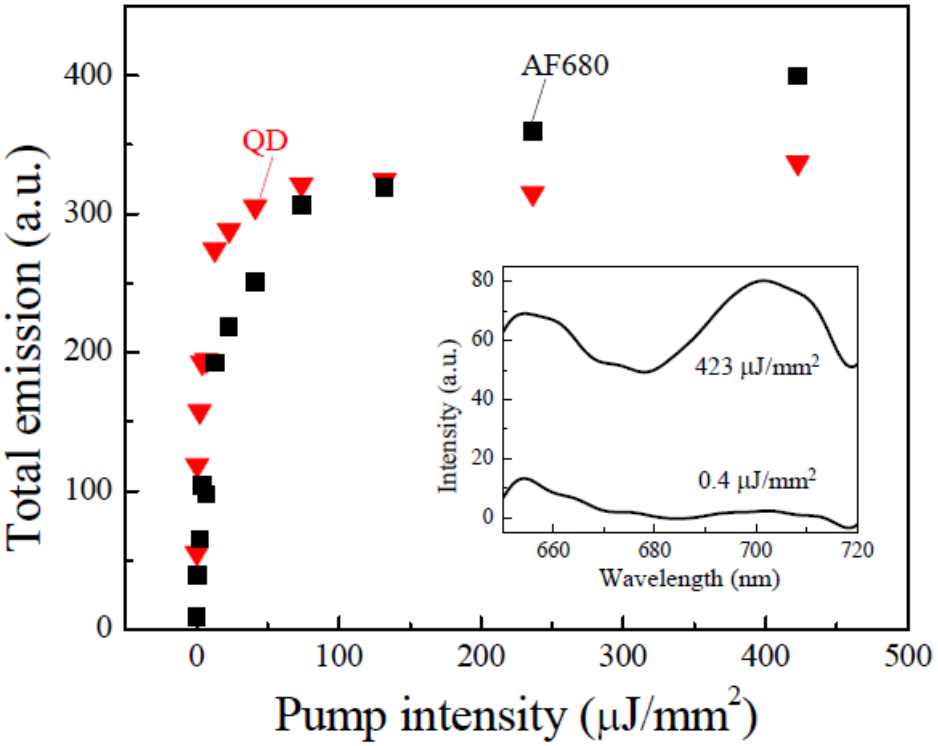

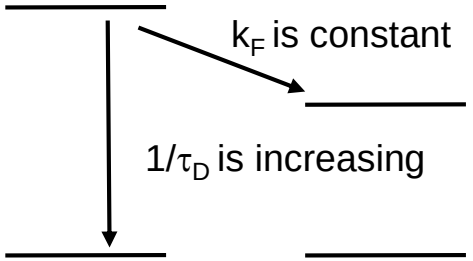

Conclusions 3

- FRET lasing can be achieved by a suitable QD-Dye FRET pair, choosing a very short distance between QD and dye, and increasing the labelling ratio.

- It is important to suppress the non-radiative Auger recombination rate of multi-exciton stated of QDs to enable FRET. This can be achieved with better surface chemistry and the use of Type II QDs.

- First FRET lasing demonstration with QDs

Q. Chen, A. Kiraz, and X Fan, Lab on a Chip (2016),

Conclusions 3

- FRET lasing can be achieved by a suitable QD-Dye FRET pair, choosing a very short distance between QD and dye, and increasing the labelling ratio.

- It is important to suppress the non-radiative Auger recombination rate of multi-exciton stated of QDs to enable FRET. This can be achieved with better surface chemistry and the use of Type II QDs.

- First FRET lasing demonstration with QDs

Q. Chen, A. Kiraz, and X Fan, Lab on a Chip (2016),

Outline

Optofluidic Lasers

- Potential of optofluidic lasers for biosensing
- Optofluidic lasing with aqueous quantum dots
- Optofluidic FRET lasing with aqueous quantum dots as donors

Gas Sensing With Elastic Microresonators

- Humidity sensinf with polymer microdisk microresonators
- Hydrogen sensing with polymer microdisk microresonators

Sensor Design & Operation Principle

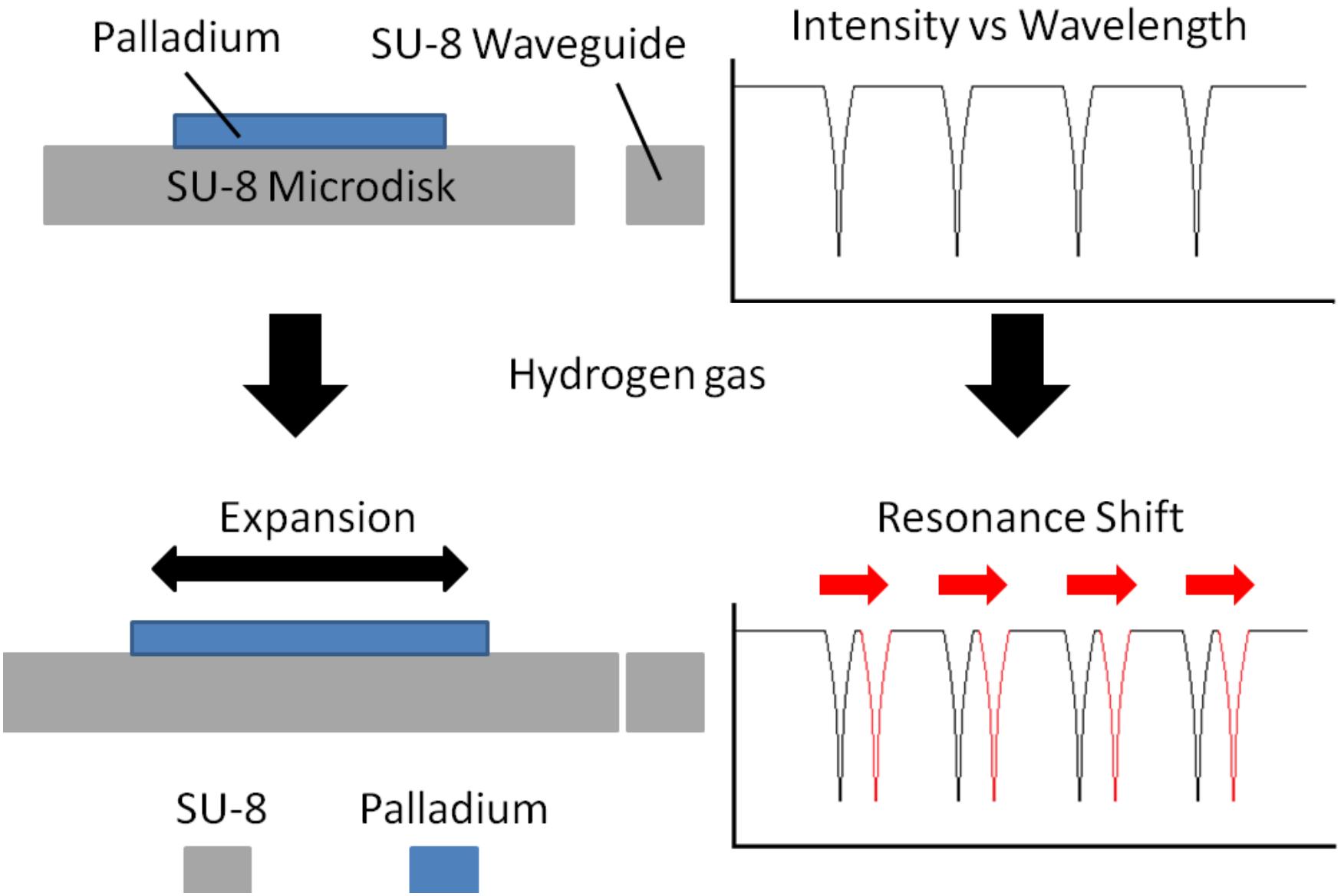

Microfabrication

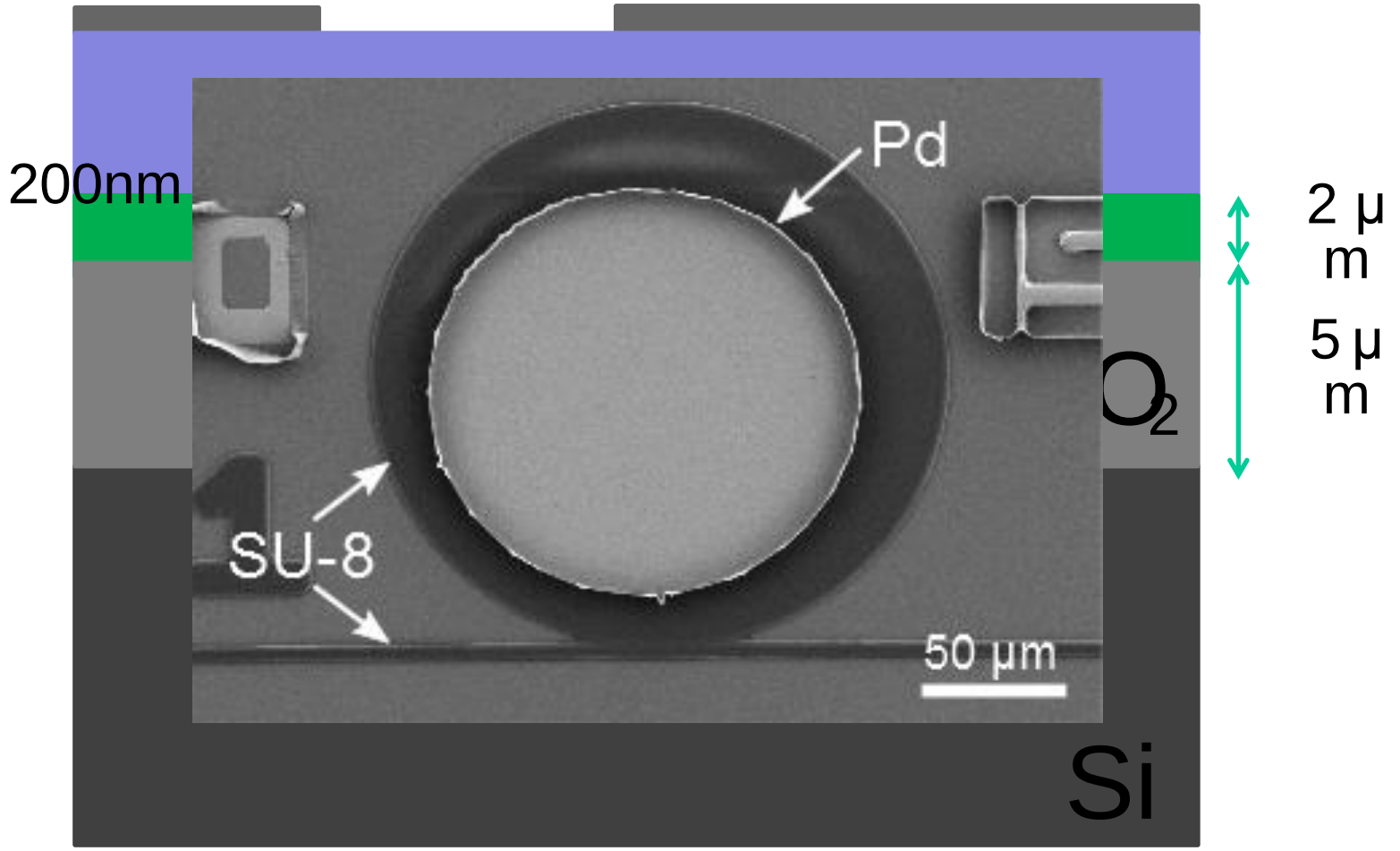

Images of Fabricated Devices

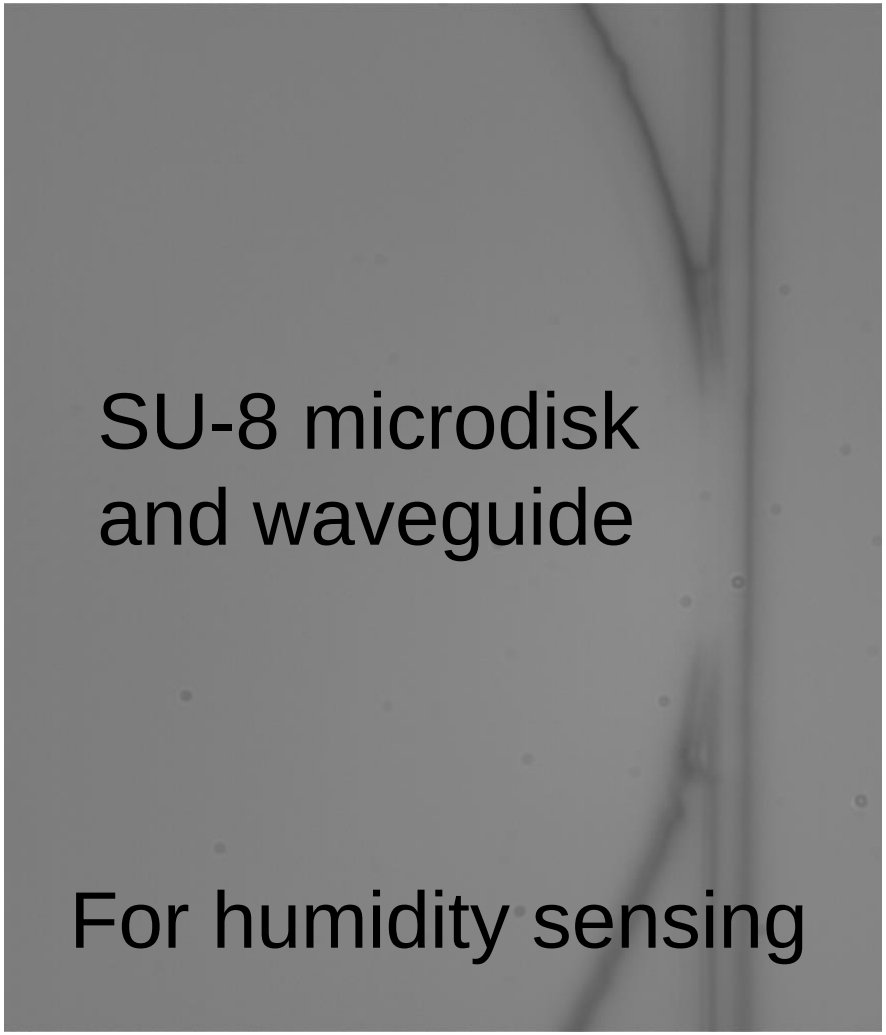

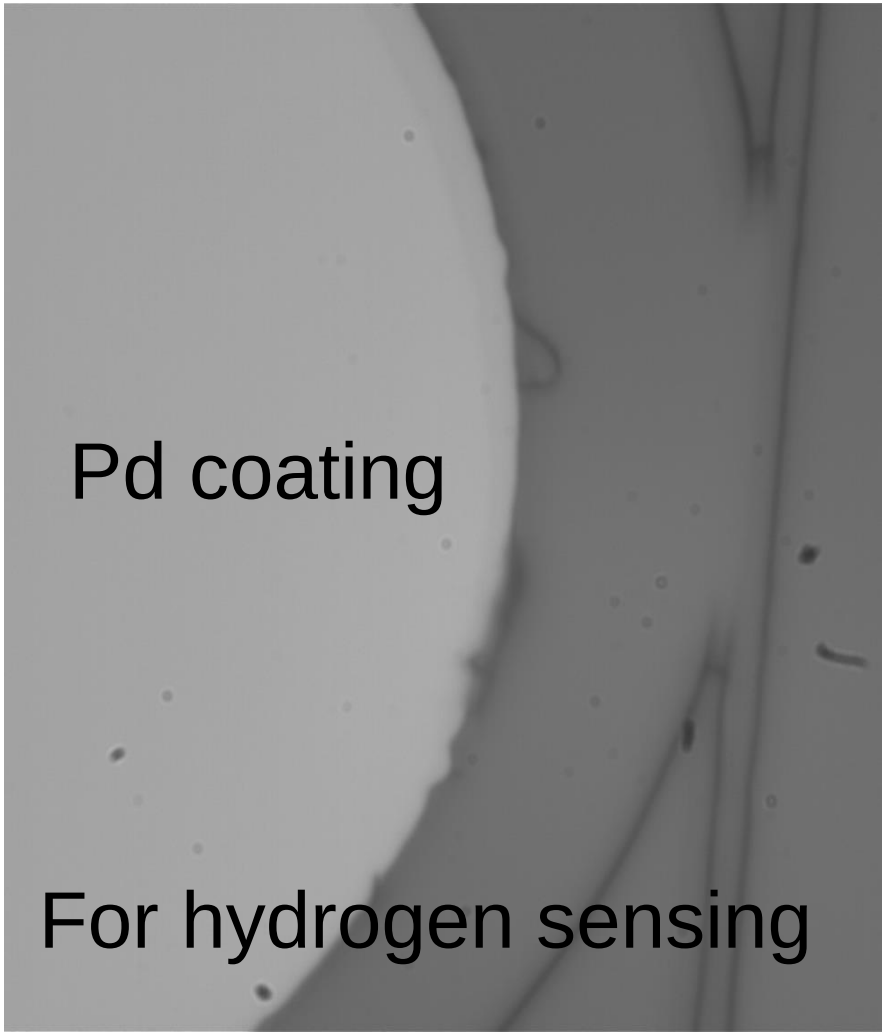

25 μm

Hydrogen Sensing Results

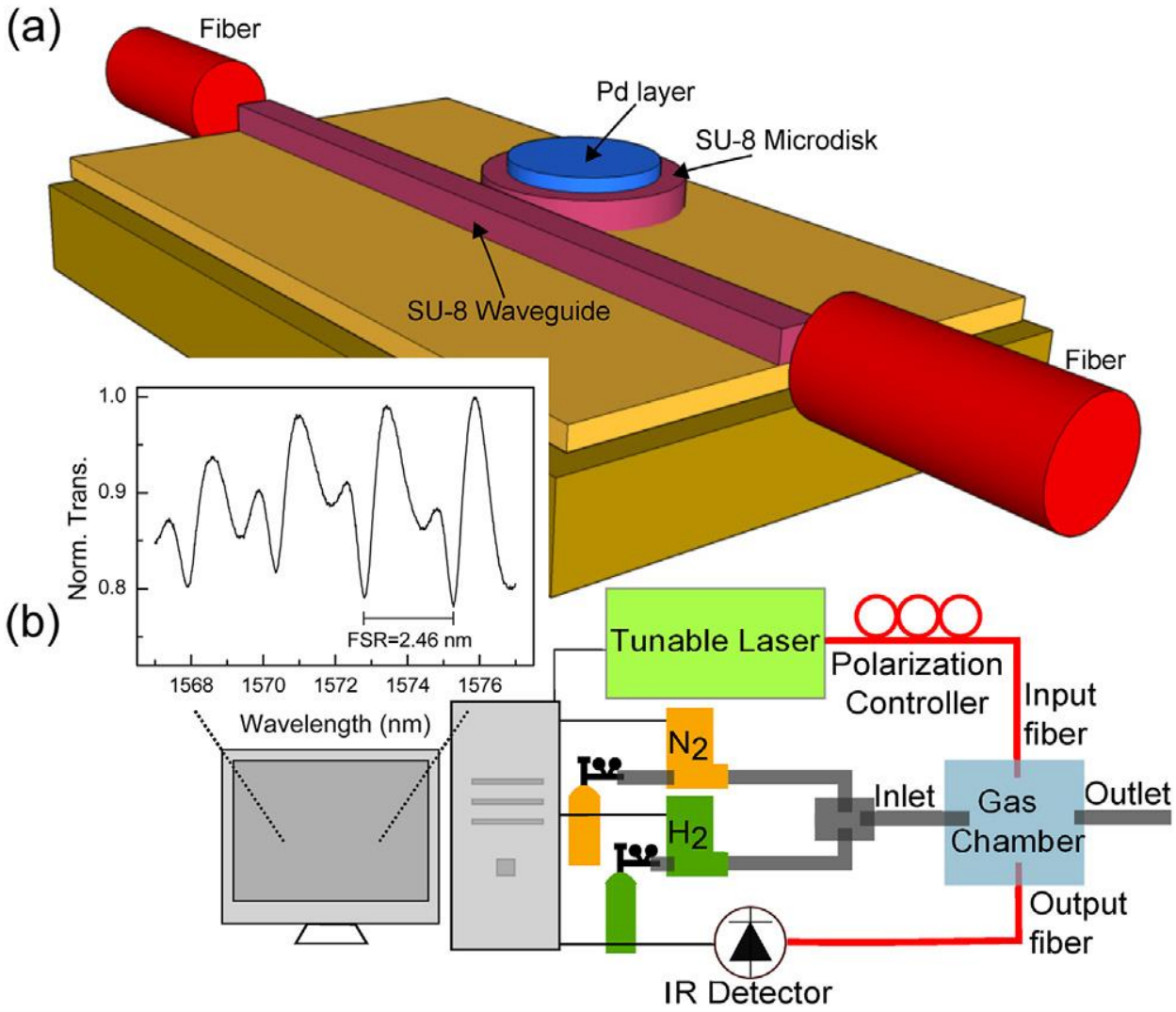

M. Eryürek et. al. Sens. and Act. B-Chem. **212**, 78-83 (2015)

Hydrogen Sensing Results

Uncoated sensor response

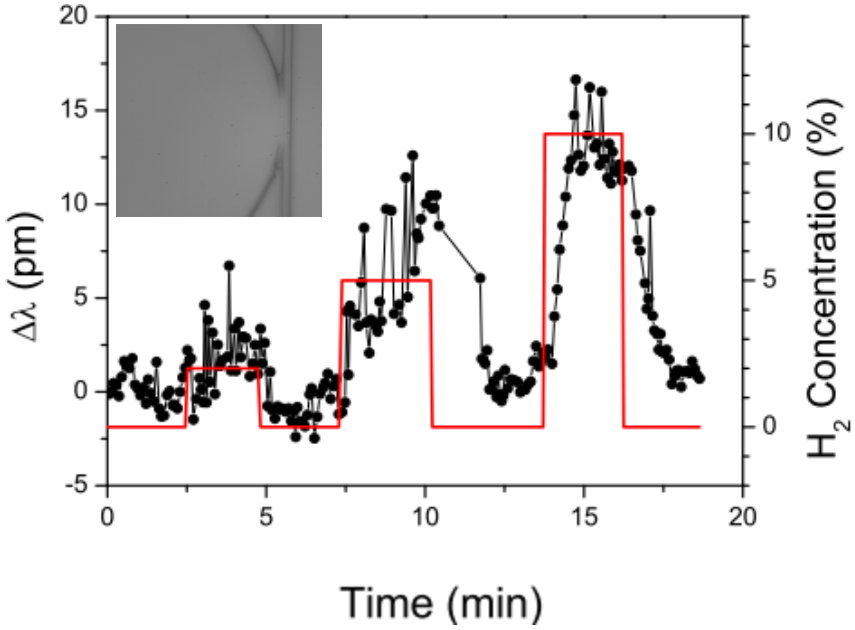

Pd coated sensor response

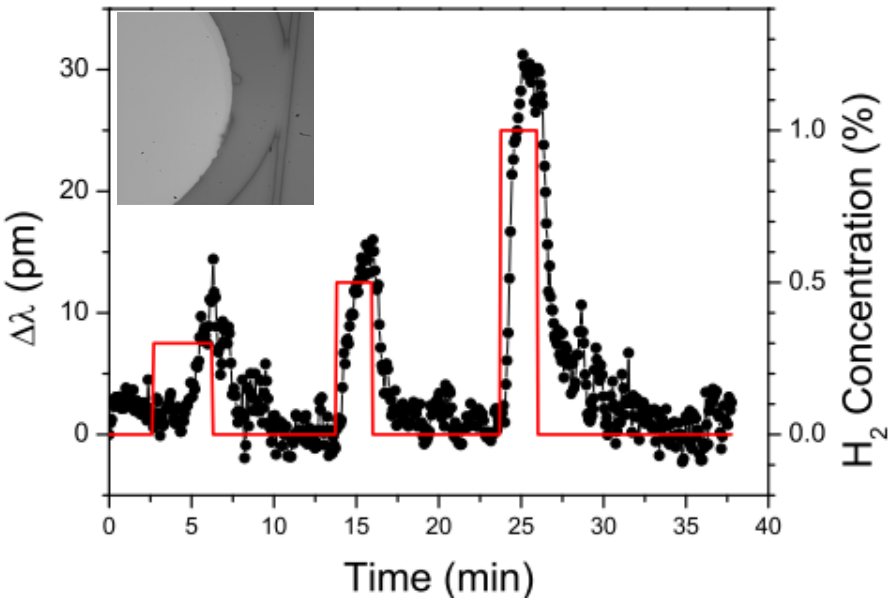

3000 ppm (0.3%) H_2 minimum detection limit
32 pm/%H2 spectral shift sensitivity

M. Eryürek et. al. Sens. and Act. B-Chem. **212**, 78-83 (2015)

Hydrogen Sensing Results

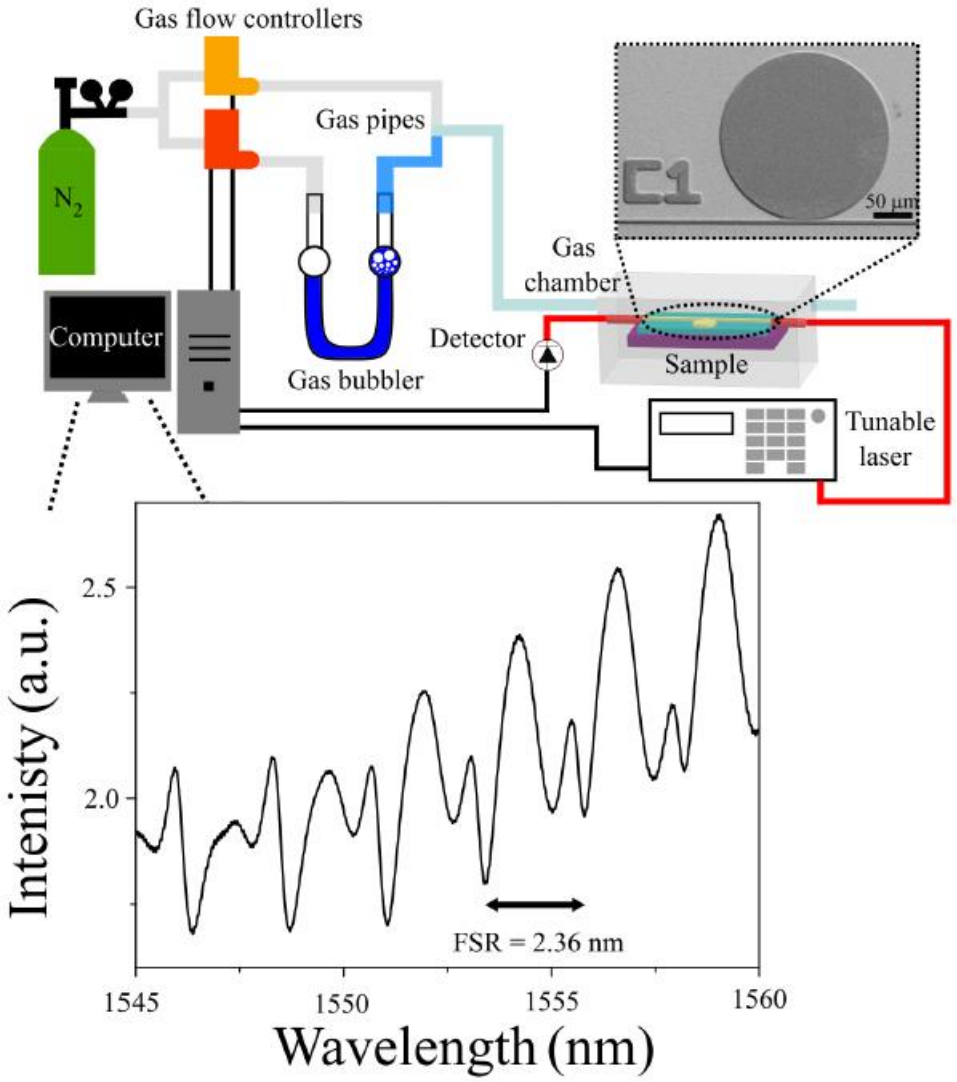

Hydrogen Sensing Results

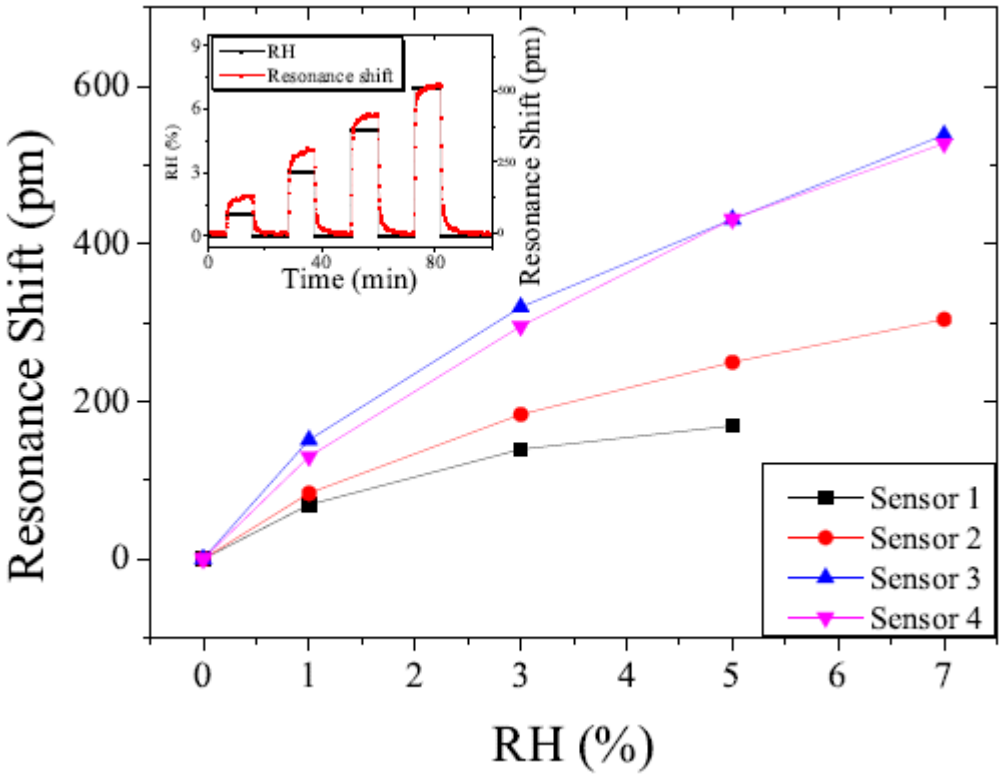

50-150 pm/%RH spectral shift sensitivity

Hydrogen Sensing Results

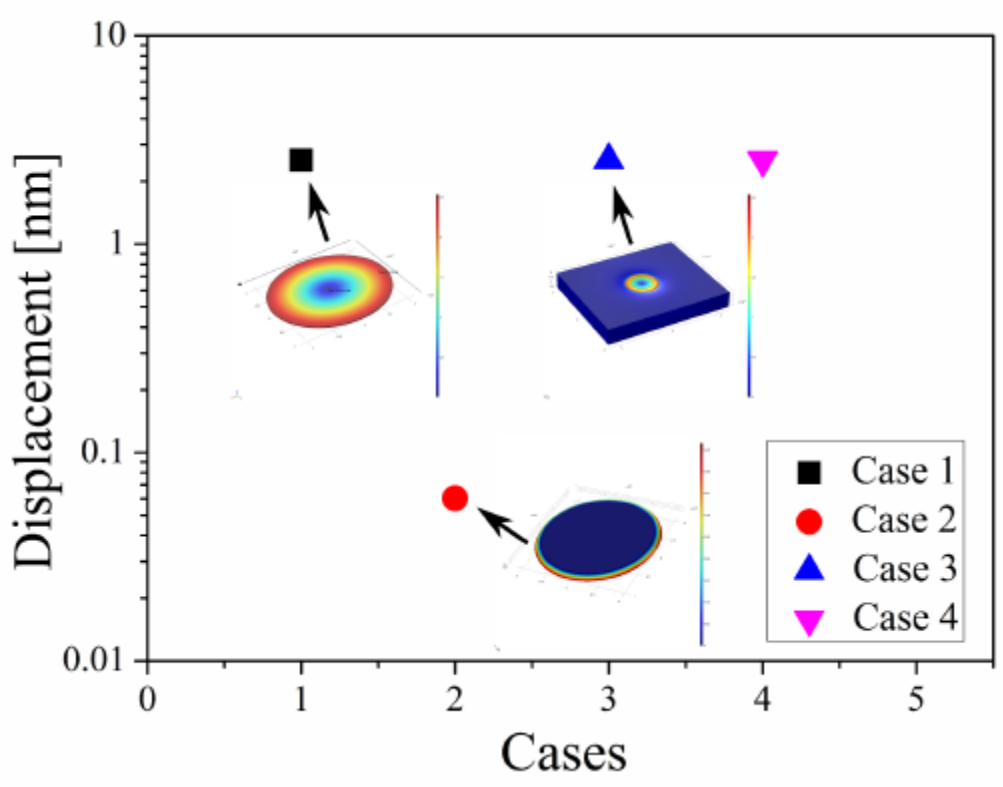

$$\frac{\Delta\lambda}{\lambda} = \frac{\Delta n}{n} + \frac{\Delta R}{R}$$

From measurements

$$\Delta n/n = 7.55 \times 10^{-5}/\%\mathrm{RH}.$$

From FEM simulaitons

$$\Delta R/R = 8 \times 10^{-7}/\%RH$$

Spectral shift is mainly due to refractive index change

Collaboration with Prof. B. E. Alaca and Z. Taşdemir, Koç U.

Conclusions 4

- 3000 ppm sensitivity to H_2 concentration is achieved 700 ppm sensitivity is predicted
- Better device fabrication for higher optical Q factors
- Sensing of other flammable (CH_4, C_3H_8) or toxic gases
- Materials research for more sensitive active layers
- Deal with the reversibility and saturation of the sensor
- Three dimensional computational analysis of compressive and shear elastic forces
- Humiditiy sensing is mainly due to refractive index change

Conclusions 4

- 3000 ppm sensitivity to H_2 concentration is achieved 700 ppm sensitivity is predicted
- Better device fabrication for higher optical Q factors
- Sensing of other flammable (CH_4, C_3H_8) or toxic gases
- Materials research for more sensitive active layers
- Deal with the reversibility and saturation of the sensor
- Three dimensional computational analysis of compressive and shear elastic forces
- Humiditiy sensing is mainly due to refractive index change

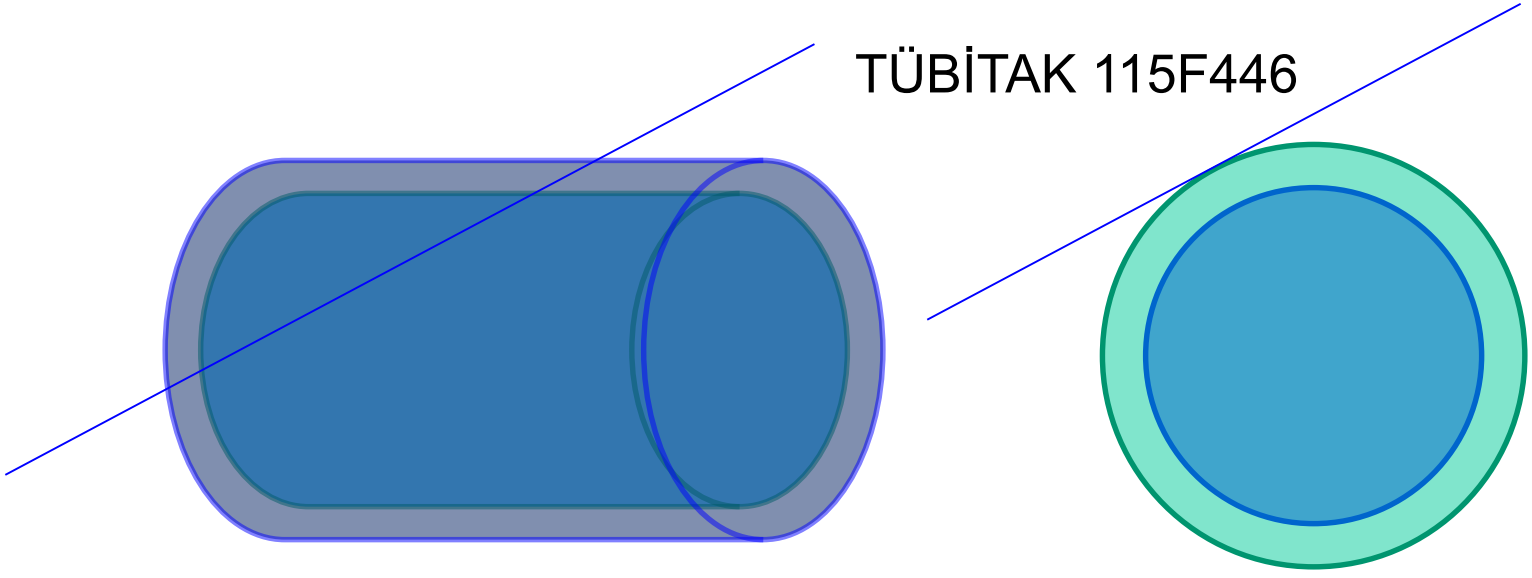

TÜBİTAK 115F446

Collaboration with Prof. V. Ötügen, SMU Dallas

Conclusions 4

- 3000 ppm sensitivity to H_2 concentration is achieved 700 ppm sensitivity is predicted
- Better device fabrication for higher optical Q factors
- Sensing of other flammable (CH_4, C_3H_8) or toxic gases
- Materials research for more sensitive active layers
- Deal with the reversibility and saturation of the sensor
- Three dimensional computational analysis of compressive and shear elastic forces
- Humiditiy sensing is mainly due to refractive index change

Thank you for listening!